ADSORPTION OF IRON (III) ION (Fe^{3+}) ON ASENI CLAY FROM KOGI STATE, NIGERIA.

BY

DAVIDSON EBUTE-METTA

PSC2105216

DEPARTMENT OF CHEMISTRY

FACULTY OF PHYSICAL SCIENCE

UNIVERSITY OF BENIN

BENIN CITY

OCTOBER, 2025

ADSORPTION OF IRON (III) ION (Fe^{3+}) ON ASENI CLAY FROM KOGI STATE, NIGERIA

BY

DAVIDSON EBUTE-METTA

PSC2105216

A PROJECT SUBMITTED TO THE

DEPARTMENT OF CHEMISTRY IN PARTIAL FULFILMENT OF THE REQUIREMENTS FOR THE AWARD OF BACHELOR OF SCIENCE (B.Sc.)

UNIVERSITY OF BENIN

BENIN CITY

OCTOBER 2025

CERTIFICATION

This is to certify that this research project was duly conducted by **EBUTE-METTA DAVIDSON** of the **Department of Chemistry**, **Faculty of Physical Sciences**, **University of Benin, Benin City**, in partial fulfillment of the requirements for the award of the **Bachelor of Science (B.Sc.) Degreein Chemistry**.

---------- ----------

DAVIDSON EBUTE-METTA Date

---------- ----------

Dr. C. A. UNUIGBE Date

(Project Supervisor)

---------- ----------

Prof. E. E. I IRABOR Date

(Head of Department)

DEDICATION

This project is dedicated to the Almighty God for the gift of life, wisdom, and his unending grace upon me. It is also dedicated to my wonderful parents, Mr. and Mrs. Ebute-Metta, whose love and support have been a constant source of strength, as well as to my siblings and friends for their invaluable contributions to every aspect of my life.

ACKNOWLEDGEMENT

I am deeply grateful to the Almighty God for His wisdom, power, protection, guidance, and love, and most especially for the priceless gift of life and the grace to successfully complete my B.Sc. programme in this great institution.

My sincere appreciation goes to my supervisor, Dr. C. A. Unuigbe, for her dedicated supervision, valuable corrections, and insightful guidance throughout the course of this research. His patience, encouragement, and commitment were instrumental to the success of this work.

I also wish to acknowledge the Head of Department, Prof. E. E. I. Irabor and all lecturers and laboratory technicians in the Department of Chemistry, particularly Mr. Clinton and Mr. Amayo, for their assistance and support.

My heartfelt gratitude goes to my loving parents, Mr. and Mrs. Ebute-Metta, for their unwavering love, care, guidance, and encouragement, as well as to my family—where I first learned the true meaning of love. Special thanks also to my beloved siblings, uncles, and aunts for their constant support.

Finally, I sincerely appreciate all my friends; Agbonifo Joseph, Chidiebere Emmanuel, Dako Karenhappuch, Efosa Goodness, Ibude Precious, Chinanu Anita, Moses Felix, Dorcas and many others for their encouragement, friendship, and immense support throughout this journey.

TABLE OF CONTENT

CHAPTER 2

CHAPTER THREE

ABSTRACT

Aseni clay was obtained from Kogi State, Nigeria. Adsorption studies of Iron (III) ions (Fe^{3+}) was carried out on the clay and Atomic Absorption Spectrometry (AAS) was employed in analysis of equilibrium concentration of Fe^{3+} ions in aqueous solution. Batch experiment involving varied initial concentration adsorbent dosage, contact time and pH were conducted. Equilibrium data showed that as initial Fe^{3+} concentration increased from 10 to 50 $mg \cdot L^{-1}$ the adsorption capacity increased from 0.96 to 3.62 $mg \cdot g^{-1}$ while percentage removal decreased from 95.7% to 72.4%, indicating progressive site saturation at higher loadings. Increasing the adsorbent mass from 0.2 to 1.0 g (per 100 mL) improved removal efficiency from 57.67% to 83.23%, demonstrating the positive effect of greater available surface sites. Contact time produced rapid initial uptake, with the amount adsorbed rising from 22.97 $mg \cdot L^{-1}$ at 5 min to 26.03 $mg \cdot L^{-1}$ at 120 min and percentage removal from 76.57% to 86.77%, indicating approach to equilibrium within the experimental timeframe. pH trials (4–9, initial concentration 100 $mg \cdot L^{-1}$) returned very high removal (>99%); however, experimental notes indicated Fe hydrolysis/precipitation during base addition which likely affected measured concentrations and must be considered when interpreting pH-dependent results. Equilibrium modelling revealed strong fits to both Langmuir and Freundlich isotherms, with a marginally better fit to the Freundlich model (R^2 = 0.9815 versus Langmuir R^2 = 0.979), consistent with adsorption on a heterogeneous surface. Kinetic analysis showed that the pseudo-second-order model provided an excellent description of the adsorption behaviour (linear t/qt versus t relationship; very high R^2), suggesting that chemisorption and surface complexation are dominant rate-controlling steps. The findings indicate that Aseni clay is a viable, low-cost adsorbent for Fe^{+3} removal under the tested laboratory conditions, especially at low to moderate contaminant concentrations, while highlighting the need for care in pH control to avoid precipitation artefacts and for further work on regeneration and real-waste testing.

LIST OF TABLES

LIST OF FIGURES

LIST OF ABBREVIATIONS AND SYMBOLS

AAS – Atomic Absorption Spectroscopy

FTIR – Fourier Transform Infrared Spectroscopy

HCL – Hollow Cathode Lamp

PMT – Photomultiplier Tube

TOT – Tetrahedral–Octahedral–Tetrahedral (2:1 clay structure)

TO – Tetrahedral–Octahedral (1:1 clay structure)

CEC – Cation Exchange Capacity

BET – Brunauer–Emmett–Teller

XRD – X-ray Diffraction (for structural analysis)

SEM – Scanning Electron Microscopy

TEM – Transmission Electron Microscopy

Fe – Iron

Fe^{2+} – Ferrous ion (Iron in +2 oxidation state)

Fe^{3+} – Ferric ion (Iron in +3 oxidation state)

$FeCl_3 \cdot 6H_2O$ – Iron(III) chloride hexahydrate

$Fe(OH)_3$ – Ferric hydroxide (iron hydroxide precipitate)

Fe_2O_3 – Ferric oxide

Fe_3O_4 – Magnetite

FeO – Ferrous oxide

FeS – Iron(II) sulfide

$[Fe(H_2O)_6]^{3+}$ – Hexaaquairon(III) complex ion

HCl – Hydrochloric acid

NaOH – Sodium hydroxide

H_2O – Water

H^+ – Hydrogen ion (proton)

OH^- – Hydroxide ion

$FeCl_2$ – Iron(II) chloride

$Fe_2O_3 \cdot xH_2O$ – Hydrated ferric oxide

rpm – Revolutions per minute (shaking speed)

pH – Potential of hydrogen

q_e – Adsorption capacity at equilibrium ($mg \cdot g^{-1}$)

q_t – Adsorption capacity at time t ($mg \cdot g^{-1}$)

q_{max} – Maximum monolayer adsorption capacity ($mg \cdot g^{-1}$)

C_0 – Initial concentration of adsorbate in solution ($mg \cdot L^{-1}$)

C_e – Equilibrium concentration of adsorbate ($mg \cdot L^{-1}$)

C_t – Concentration of adsorbate at time t ($mg \cdot L^{-1}$)

Ca – Amount of adsorbate removed or adsorbed ($mg \cdot L^{-1}$)

V (L) – Volume of solution in litres

m – Mass of adsorbent (g)

k_1 – Pseudo-first-order rate constant (min^{-1})

k_2 – Pseudo-second-order rate constant ($g \cdot mg^{-1} \cdot min^{-1}$)

K_L – Langmuir isotherm constant related to binding affinity ($L \cdot mg^{-1}$)

K_F – Freundlich isotherm constant related to adsorption capacity

1/n – Freundlich heterogeneity factor (indicates surface heterogeneity; $0 < 1/n < 1$ = favorable adsorption)

R^2 – Coefficient of determination

% Removal – Percentage of metal ion removed from solution

t/q_t – Linearized form variable used in pseudo-second-order model

$\ln(q_e - q_t)$ – Logarithmic expression in pseudo-first-order kinetics

CHAPTER 1

1.1 **Introduction**

The problem of heavy metal pollution has become a global environmental concern, with toxic metals accumulating in soil, water, and the food chain. Elements such as iron (Fe), lead, cadmium and arsenic occur naturally at low levels, but human activities (mining, smelting, agriculture, etc.) release them in excess (Onakpa *et al.,* 2018; Nkwunonwo *et al.,* 2020). Because heavy metals do not biodegrade and tend to bioaccumulate, even modest increases can poison ecosystems and human health (Nkwunonwo *et al.,* 2020). In Nigeria, a rapidly growing, industrializing country, heavy metal levels in soils and crops are already elevated. For example, studies around Kogi State's Itakpe iron mine report higher concentrations of several metals in local crops than in control areas (Onakpa *et al.,* 2018). These findings highlight how mining and other activities can disperse metals like Fe into surrounding soils and food systems, making pollution control urgent.

Heavy metals released into the environment migrate through multiple pathways. Contaminants in soil can be taken up by plant roots or leached into groundwater, while metals in water can settle into sediments. Atmospheric dust or fumes (from steelmaking, power plants, vehicles, etc.) carry metals that eventually deposit on land or water. This "multi-media" pollution means an excess of Fe or other metals in one compartment often impacts others. Crops grown on contaminated soil or irrigated with polluted water can accumulate metals, passing them up the food chain. In Nigeria, vegetables and staple grains have been shown to contain dangerous levels of lead, cadmium, and iron, underscoring links between environmental contamination and food safety. In short, heavy metals like Fe persist in air, soil and water and ultimately enter ecosystems and diets (Nkwunonwo *et al.,* 2020 ; Onakpa *et al.,* 2018).

Recent studies show that excessive dissolved iron in aquatic environments can lead to ecotoxicological effects: for example, chronic exposure to high concentrations of Fe(III) under varying pH, hardness, and dissolved organic carbon causes toxicity in algae, invertebrates and fish, sometimes exceeding solubility limits and causing precipitation of iron hydroxides that impair gill function and reduce oxygen transport (Environmental Toxicology and Chemistry, 2023). Similarly, Fe-DTPA exposure in catfish has been shown to impact gill health, breathing efficiency, and metabolic stress (Hildebrand *et al.,* 2023). In soils, excess ferrous iron (Fe^{+2}) in flooded or acidic fields leads to direct phytotoxicity. For instance, in waterlogged rice paddies with high dissolved iron, plants show leaf bronzing and stunted growth, causing serious yield losses (Li *et al.,* 2019). These effects illustrate that iron pollution impacts ecosystems beyond water – it harms aquatic life and crops alike.

Overall, iron contamination contributes to a broader burden of heavy metals on the environment. Excess Fe in soils can tie up phosphorus and other nutrients, degrade soil microbes and reduce fertility, while iron dust from industrial activity lowers air quality. In Nigeria's Middle Belt (e.g. Kogi State), iron mining has already been linked to raised soil metal levels. Thus iron, like other heavy metals, threatens soil health, agricultural productivity and ecosystem balance if unchecked. This situation motivates the search for practical, local solutions to bind and remove Fe from the environment.

One promising approach is adsorption using natural materials. Among remediation techniques, adsorption is attractive because it is simple, cost-effective and scalable. Clay minerals in particular are excellent adsorbents: they are low-cost, widely available, and have a layered silicate structure with a very high surface area and cation-exchange capacity. These properties enable clays to bind metal ions strongly across a range of conditions. Recent reviews note that both raw and treated clays (kaolinite,

montmorillonite, bentonite, etc.) can effectively remove heavy metals such as lead, cadmium, arsenic and iron from water and soils (Wang *et al.,* 2024). In Nigeria, experimental studies have confirmed that local clays can serve as heavy-metal sponges: for example, an unmodified Nigerian kaolinite was shown to adsorb substantial amounts of Pb^{2+} and Cd^{2+}, and acid activation further increased its surface area and uptake capacity. Such findings suggest that natural clay deposits which are abundant in many parts of Nigeria could be tapped as low-cost adsorbents to clean up metal pollution.

The focus of this work is on Aseni Clay (2nd Layer), a locally available clay deposit in Kogi State, Nigeria. Geologically, Aseni clay is a phyllosilicate material rich in silica and alumina, implying a high density of adsorption sites (Wang *et al.,* 2024). Preliminary characterization indicates Aseni clay has a very large BET surface area (on the order of 170 m^2/g) and is composed mainly of silicate minerals. These attributes suggest it could effectively trap iron ions from solution. Using Aseni clay for Fe removal leverages a material that is locally abundant and cheap, aligning with sustainable remediation goals. By investigating Aseni clay's ability to adsorb iron, this study seeks a practical way to mitigate heavy metal contamination using indigenous resources.

1.1.1 Background of the Study

Heavy metals are generally defined as dense metallic elements that pose toxicological risks even at low concentrations. Common heavy metals include lead (Pb), cadmium (Cd), chromium (Cr), mercury (Hg) and iron (Fe). Although trace amounts of many of these metals are essential for life, anthropogenic activities have greatly increased their environmental loading. In Nigeria, large-scale mining (of iron, tin, gold, etc.), industrial emissions, and the use of agrochemicals have introduced heavy metals into soils, waters

and the atmosphere. These pollutants are non-degradable and tend to accumulate in sediments and soils over time. As a result, even remote areas can become sinks for metals that were long ago emitted nearby or transported by rivers and wind.

Once in the environment, heavy metals cycle through soil, water, air and the biosphere. Plants absorb metals from contaminated soils, and animals take them up through food and water. This leads to bioaccumulation and biomagnification, higher concentrations in organisms at upper food-chain levels. In Kogi State (home to the Aseni deposit), studies have reported elevated heavy metal contents in crops grown near iron mining sites, indicating that local farming systems are already impacted. Human exposure occurs mainly through ingestion (contaminated food and water) and inhalation (dust and aerosols). For example, toxic metals deposited on vegetable farms can end up in spices and crops, posing health hazards to consumers (Onakpa *et al.,* 2018). Furthermore, iron in excess can disrupt biochemical processes: in waterlogged soils it injures plant roots, while in the human body it can catalyze free radical formation if ingested in large amounts. In sum, heavy metal pollution, including that of iron is a multifaceted problem that spans agriculture, water resources and public health.

Because heavy metals are persistent, remediation is challenging. Traditional methods (chemical precipitation, ion exchange, phytoremediation) can be costly or slow. Adsorption has emerged as an efficient and practical alternative. In adsorption, dissolved metal ions adhere to solid surfaces, which can then be removed from the system. Clays and other natural materials have been widely studied as adsorbents because they are non-toxic and inexpensive. For instance, untreated Nigerian kaolinite clay has been shown to bind lead, cadmium and nickel from solution, and activating the clay with dilute acid markedly enhanced its uptake capacity. These results demonstrate that even unmodified clays possess useful adsorption sites, and

that their performance can be tuned by relatively simple treatments. In practical environmental cleanup, using the raw (or lightly treated) clay directly is appealing for its simplicity.

Prior research thus motivates the present study of Aseni clay for iron removal. Aseni clay's mineralogy (dominated by silica and alumina layers) is typical of clays known to adsorb metal ions. Its high measured surface area (approximately 171 m^2/g) and fine particle structure imply many active binding sites. However, despite these promising traits, Aseni clay has not been systematically tested for heavy metal adsorption in the scientific literature. This gap is notable because Aseni is locally abundant, and an effective use would offer a sustainable way to clean up iron pollution using Nigerian resources. Therefore, this study will fill that gap by examining how well Aseni clay (2nd layer) adsorbs dissolved Fe, thereby addressing both a fundamental environmental problem and a practical remediation need.

1.1.2 Statement of the Problem

The presence of heavy metals in the environment poses serious ecological and public health concerns. Iron (Fe), although considered an essential element for biological systems, becomes toxic when present in excess. Elevated levels of iron in the environment have been associated with reduced soil fertility, toxicity to plants, contamination of food crops, and oxidative damage in biological systems (Mahender *et al.,* 2019).

Areas surrounding mining and metal-processing zones often exhibit higher concentrations of iron in soils and crops, raising concerns about long-term contamination (Onakpa *et al.,* 2018). Communities in proximity to these sources are particularly at risk due to the potential for iron to accumulate in food systems, surface deposits, and household water. Unfortunately, access to effective remediation tools in many of these communities remains limited

(Nkwunonwo *et al.,* 2020).

Traditional methods for heavy metal removal from the environment, such as chemical precipitation and ion exchange, are often expensive and technically demanding, making them less feasible in low-resource settings. Furthermore, these techniques may introduce secondary pollutants or require extensive infrastructure. This creates a need for simple, low-cost, and environmentally friendly solutions that can address heavy metal pollution effectively (Wang *et al.,* 2024).

Natural clay minerals offer promising alternatives due to their abundance, low cost, and natural adsorptive capacity. However, while various types of Nigerian clays have been explored in past studies, there is a lack of documented research on the potential of Aseni Clay, particularly the second layer, for iron adsorption. The performance of this clay in adsorbing iron ions has not been clearly established. Therefore, this study seeks to fill that knowledge gap by investigating the adsorption efficiency of Aseni Clay (2nd Layer) for iron removal, providing data that could support the development of accessible remediation techniques in affected environments.

1.1.3 Justification of the Study

Heavy metal contamination has become a critical environmental challenge due to rapid industrialization, mining activities, agricultural practices, and improper waste management. Among these metals, iron occupies a unique position as both an essential micronutrient and a pollutant when present in excess. While moderate concentrations of iron are necessary for plant growth, soil fertility, and human health, excessive accumulation of this metal has been linked to ecological imbalance, reduced agricultural productivity, and public health risks (Mahender *et al.,* 2019).

Conventional technologies for the removal of heavy metals, such as chemical

precipitation, membrane filtration, ion exchange, and electrochemical treatment, though effective, are often associated with high operational costs, complexity, and the generation of secondary waste (Kumar, 2024).

These limitations render such methods impractical in many low-income or rural communities, including those in Nigeria, where industrial discharges and artisanal mining activities significantly elevate environmental metal burdens. Therefore, the search for cost-effective, eco-friendly, and readily available alternatives has gained substantial research interest.

Clay minerals, due to their abundance, affordability, and high surface activity, represent one of the most promising natural adsorbents for heavy metal remediation. Nigerian clays, in particular, are widely distributed and locally accessible, making them suitable candidates for sustainable environmental management strategies (Adebowale *et al.,* 2006). However, while studies have investigated kaolinite and other common clays, limited research has been dedicated to Aseni Clay, especially the second layer, whose mineralogical properties may offer unique advantages for iron adsorption. Exploring its adsorption potential therefore fills a knowledge gap and expands the database of indigenous clays applicable to remediation purposes.

This study is justified by the dual necessity of addressing a pressing environmental concern, heavy metal contamination and promoting the utilization of indigenous materials. By demonstrating the efficiency of Aseni Clay (2nd Layer) in adsorbing iron from contaminated systems, this research may provide a foundation for developing low-cost, scalable, and sustainable remediation techniques. Furthermore, the work will contribute to academic literature and serve as a scientific resource for future industrial and environmental policy formulation in Nigeria.

1.1.4 Scope of the Study

This investigation focuses on the assessment of Aseni Clay (second layer) as an adsorbent for the removal of Fe^{3+} ions from aqueous matrices. The scope of the study begins with the collection and processing of the Aseni clay sample to ensure it is suitable for adsorption experiments.

The clay will undergo physicochemical characterization, including the determination of surface area, pore morphology, functional groups, and cation exchange capacity. These properties are essential for understanding the adsorption mechanism and for establishing correlations between surface characteristics and adsorption efficiency.

The study further involves batch adsorption experiments conducted under controlled laboratory conditions, aimed at evaluating the effect of critical operational parameters such as initial Fe^{3+} concentration, contact time, adsorbent dosage, pH, and thermal conditions on adsorption performance.

To gain deeper insight into the adsorption behavior, adsorption isotherm models—specifically Langmuir, Freundlich, Temkin, and Dubinin–Radushkevich will be applied to model the equilibrium data. Additionally, kinetic studies will be carried out to elucidate the adsorption mechanisms and rate-controlling steps.

Finally, the study will assess the practical viability of Aseni clay as a cost-effective adsorbent for water purification, thereby contributing to the development of sustainable and locally available solutions for heavy metal remediation.

1.1.5 Aim and Objectives

Aim

The aim of this study is to investigate the adsorption potential of **Aseni Clay (2nd Layer)** for the removal of iron (Fe^{3+}) ions from aqueous solutions under

controlled laboratory conditions.

Objectives

To achieve this aim, the study will pursue the following objectives:

- To collect and prepare Aseni Clay for use as an adsorbent.
- To evaluate the effect of operational parameters such as pH, adsorbent dosage, contact time, and initial metal concentration on the adsorption of Fe^{3+} ions.
- To model adsorption equilibrium data using isotherm models (Langmuir, Freundlich).
- To investigate the adsorption kinetics and mechanisms involved in the removal of Fe^{3+} ions.
- To assess the potential of Aseni Clay as a low-cost and sustainable material for water treatment applications.

1.2 LITERATURE REVIEW

1.2.1 Heavy Metals and Environmental Impact

1.2.1.1 Definition of Heavy Metals

Heavy metals are naturally occurring metallic elements characterized by relatively high atomic weight and density, typically greater than 5 g/cm³, and their tendency to exhibit toxic effects even at low concentrations. They include both essential elements such as iron (Fe), zinc (Zn), and copper (Cu), which are required for metabolic and physiological functions, as well as non-essential toxic elements such as cadmium (Cd), lead (Pb), and mercury (Hg), which have no biological role and are harmful even in trace amounts (Jomova *et al.,* 2024).

A defining characteristic of heavy metals is their environmental persistence. Unlike organic pollutants that can be degraded through microbial or photochemical processes, heavy metals are non-biodegradable and remain in circulation within soil, water, air, and living organisms for long periods. This persistence leads to accumulation and long-term ecological and health risks (He *et al.,* 2024).

Another key feature is their ability to bioaccumulate and biomagnify. Even at very low concentrations in soil or water, heavy metals can be absorbed by plants, transferred to animals through the food chain, and eventually reach higher concentrations in humans, where they induce oxidative stress, inhibit enzymes, and disrupt essential metabolic pathways (Jomova *et al.,* 2024).

Sources of heavy metals include both natural and anthropogenic inputs. Natural sources consist of volcanic eruptions, weathering of rocks, and soil erosion, while anthropogenic sources such as mining, smelting, fossil fuel combustion, agricultural chemicals, and industrial effluents contribute more significantly to harmful environmental levels (Abd Elnabi *et al.,* 2023). This dual origin reinforces the importance of defining heavy metals not only by their physical properties but also by their ecological persistence, toxicity, and significance as global pollutants.

1.2.1.2 Characteristics of Heavy Metals

Heavy metals share several defining characteristics that make them significant in environmental science and toxicology. These include their physical properties, persistence, bioaccumulation potential, and biological impacts.

- **High Density and Atomic Weight**

  Heavy metals typically have densities greater than 5 g/cm³ and relatively high atomic weights. These physical characteristics distinguish them from lighter metals and contribute to their environmental behavior (Jomova *et al.,* 2024).

- **Persistence in the Environment**

  Unlike organic pollutants, heavy metals are not biodegradable. Once introduced into ecosystems, they persist for decades or centuries, cycling between soil, water, air, and living organisms without undergoing natural breakdown (He *et al.,* 2024).

- **Toxicity at Low Concentrations**

  While some metals such as Fe, Zn, and Cu are essential micronutrients, they become toxic when concentrations exceed physiological thresholds. Non-essential metals such as Cd, Pb, and Hg exhibit toxicity even at very low levels, impairing biochemical and metabolic processes (Abd Elnabi *et al.,* 2023).

- **Bioaccumulation and Biomagnification**

  Heavy metals have a strong tendency to accumulate in living organisms and magnify through food chains. This means that small concentrations in soil or water can result in much higher concentrations in plants, animals, and eventually humans, leading to chronic exposure risks (Jomova *et al.,* 2024).

- **Affinity for Biological Molecules**

  Many heavy metals bind strongly to proteins, enzymes, and nucleic acids. This disrupts enzymatic functions, generates reactive oxygen

species (ROS), and induces oxidative stress that damages cells and tissues (He *et al.,* 2024).

- **Multiple Natural and Anthropogenic Sources**
  Heavy metals are released from both natural processes (volcanic eruptions, rock weathering) and human activities such as mining, smelting, fuel combustion, and the use of agrochemicals. Human contributions typically exceed natural levels and represent the main driver of environmental contamination (Abd Elnabi *et al.,* 2023).

1.2.1.3 Sources of Heavy Metals

Heavy metals enter the environment through a combination of natural processes and anthropogenic activities, but in modern times, human contributions have significantly surpassed natural background levels. Their sources can be broadly categorized as follows:

Natural Sources

- **Geological Weathering**: Weathering of rocks and soil minerals continuously releases trace amounts of metals such as Fe, Mn, and Zn into the environment. This process contributes to background concentrations in soils and water systems (He *et al.,* 2024).
- **Volcanic Activity**: Volcanic eruptions emit metals like Hg, As, and Pb into the atmosphere and surrounding ecosystems, often in concentrated pulses.
- **Atmospheric Dust and Erosion**: Desert dust storms and soil erosion redistribute metals across large distances, affecting both terrestrial and aquatic systems.

Anthropogenic Sources

- **Mining and Smelting**: Extraction and processing of ores are among the largest contributors to heavy metal pollution. Tailings, mine drainage, and atmospheric emissions release large amounts of Fe, Pb, Cd, and Cr into nearby soils and waterways (Abd Elnabi *et al.,* 2023).
- **Industrial Activities**: Metal plating, tanneries, textiles, cement, and battery production introduce diverse metals into air, wastewater, and soils.
- **Agricultural Practices**: Pesticides, phosphate fertilizers, and sewage sludge used as manure are significant sources of Cd, Pb, and Zn in farmland soils (Jomova *et al.,* 2024).
- **Fossil Fuel Combustion**: Burning coal and petroleum products emits Pb, Hg, Ni, and V into the atmosphere, which later deposit on land and water.
- **Urbanization and Waste Disposal**: Solid waste, electronic waste, and untreated municipal effluents contribute mixed heavy metals into terrestrial and aquatic environments.

Globally, anthropogenic inputs far outweigh natural sources, particularly in industrializing regions. The persistence of heavy metals ensures that once introduced, they accumulate and spread across environmental compartments, amplifying long-term risks to ecosystems and human health.

1.2.1.4 Environmental Impacts of Heavy Metals

Heavy metals are of major ecological concern because they are toxic, persistent, and capable of bioaccumulation. Unlike organic contaminants, they do not degrade into harmless forms, meaning that once released into the

environment, they remain for decades and continually cycle between soil, water, air, and living organisms. Their impacts cut across terrestrial, aquatic, and atmospheric systems, often creating long-term ecological imbalance.

Soil Ecosystems

Heavy metals accumulate in soils, where they disrupt microbial communities, reduce enzymatic activity, and impair soil fertility. Essential nutrient cycles, including nitrogen and phosphorus cycling, are negatively affected, leading to poor agricultural productivity. Crops grown in contaminated soils can take up metals such as Cd, Pb, and Fe, transferring them into the food chain (He *et al.,* 2024).

Aquatic Ecosystems

Runoff from mining, industrial effluents, and agricultural leaching introduces metals into surface waters. In aquatic systems, heavy metals such as Fe, Cu, and Pb can damage fish gills, impair reproduction, and reduce biodiversity. They also accumulate in sediments, where they act as long-term secondary sources of contamination even after direct inputs decline (Abd Elnabi *et al.,* 2023).

Air and Atmospheric Impacts

Combustion of fossil fuels and industrial processes release particulate-bound metals such as Hg, Pb, and Ni into the atmosphere. These airborne particles deposit onto soils and waters, expanding the reach of pollution beyond the original source. Long-range transport means that even remote areas far from industry can become contaminated (Jomova *et al.,* 2024).

Bioaccumulation and Food Chain Effects

One of the most severe impacts of heavy metals is their tendency to bioaccumulate in organisms and biomagnify through trophic levels. Plants absorb metals from soil and water, herbivores consume the plants, and humans

ultimately ingest metals through food and water. This process leads to chronic exposure that can result in health disorders ranging from reduced crop yield to neurological and organ damage in higher organisms.

Ecosystem Stability

Persistent heavy metal stress leads to reduced biodiversity, shifts in species dominance, and long-term ecological imbalance. For instance, high levels of Fe and other metals in soils reduce crop diversity and threaten food security, while aquatic contamination undermines fish populations and local fisheries (He *et al.,* 2024).

1.2.2 Iron as a Heavy Metal

Iron (Fe) is one of the most abundant elements in the Earth's crust and plays a dual role in environmental and biological systems. On the one hand, it is an essential micronutrient required for oxygen transport, electron transfer, and enzyme activity in plants, animals, and humans. On the other hand, excessive concentrations of iron can become toxic, particularly when linked to anthropogenic activities such as mining, metallurgy, and industrial discharge (Rastogi *et al.,* 2022).

In environmental science, iron is often grouped with heavy metals due to its high atomic mass (55.85 g/mol), relatively high density (7.87 g/cm^3), and ecological significance. Although it is not as acutely toxic as cadmium or mercury, iron contamination poses a serious risk because of its persistence, mobility, and bioavailability in soils and aquatic systems (He *et al.,* 2024). Unlike organic pollutants, excess iron cannot degrade but instead cycles between oxidation states (Fe^{2+} and Fe^{3+}), influencing redox chemistry, soil fertility, and water quality.

Excessive iron in soils has been associated with reduced crop yield, particularly in flooded or acidic conditions where ferrous iron (Fe^{2+}) becomes soluble and phytotoxic. Similarly, in aquatic environments, the precipitation of ferric hydroxides can coat fish gills and smother benthic organisms, leading to biodiversity loss (Nkwunonwo *et al.,* 2020; He *et al.,* 2024). In humans, chronic iron overload results in oxidative stress, tissue injury, and systemic diseases such as liver cirrhosis and cardiovascular complications (Camaschella, 2019; Jomova *et al.,* 2024).

Because iron is both a vital nutrient and a potential contaminant, its study occupies a central place in environmental monitoring and remediation research. Understanding the occurrence, properties, sources, and impacts of Fe provides insight into broader heavy metal pollution challenges and informs strategies such as adsorption using natural materials like clay.

1.2.2.2 General Properties of Iron(Fe)

Table 1.1

Properties	**Value / Description**
Name	Iron
Symbol	Fe
Atomic Number	26
Atomic Weight	55.845 g/mol
Density	7.87 g/cm³ (at 20°C)
Melting Point	1538 °C
Boiling Point	2862 °C

Colour	Lustrous metallic gray
Crystal Structure	Body-Centered Cubic (BCC) at room temperature
Electronic Configuration	[Ar] $3d^6$ $4s^2$
Oxidation State	+2, +3 (most common), +6 (rare)
Magnetic Properties	Ferromagnetic
Thermal Conductivity	80.2 W/m·K
Electrical Resistivity	9.71 μΩ·cm
Abundance in Earth's Crust	~5% (fourth most abundant element)

1.2.2.3 Physical Properties of Iron

Iron is a silvery-gray, lustrous metal with a density of approximately 7.87 g cm^{-3} at 20 °C, a value consistent across standard references. It has a melting point of about 1538 °C and a boiling point around 2861–2862 °C, which reflects strong metallic bonding and thermal stability (RSC, 2025).

The element exhibits classic allotropy: at ambient conditions, it exists as α-Fe (body-centered cubic), transitions to γ-Fe (face-centered cubic) above 912 °C, and reverts to δ-Fe (bcc) near 1394 °C before reaching the melting point. These transformations define its structural behavior under temperature variation (Britannica, 2025).

Magnetically, iron is ferromagnetic at room temperature and becomes paramagnetic at its Curie temperature (~770 °C; 1043 K) (Britannica, 2025).

In terms of transport properties, iron demonstrates high thermal conductivity (≈80 W m^{-1} K^{-1} at 20 °C) and low electrical resistivity (≈9.7 μΩ·cm at 20 °C), consistent with its metallic nature (RSC, 2025).

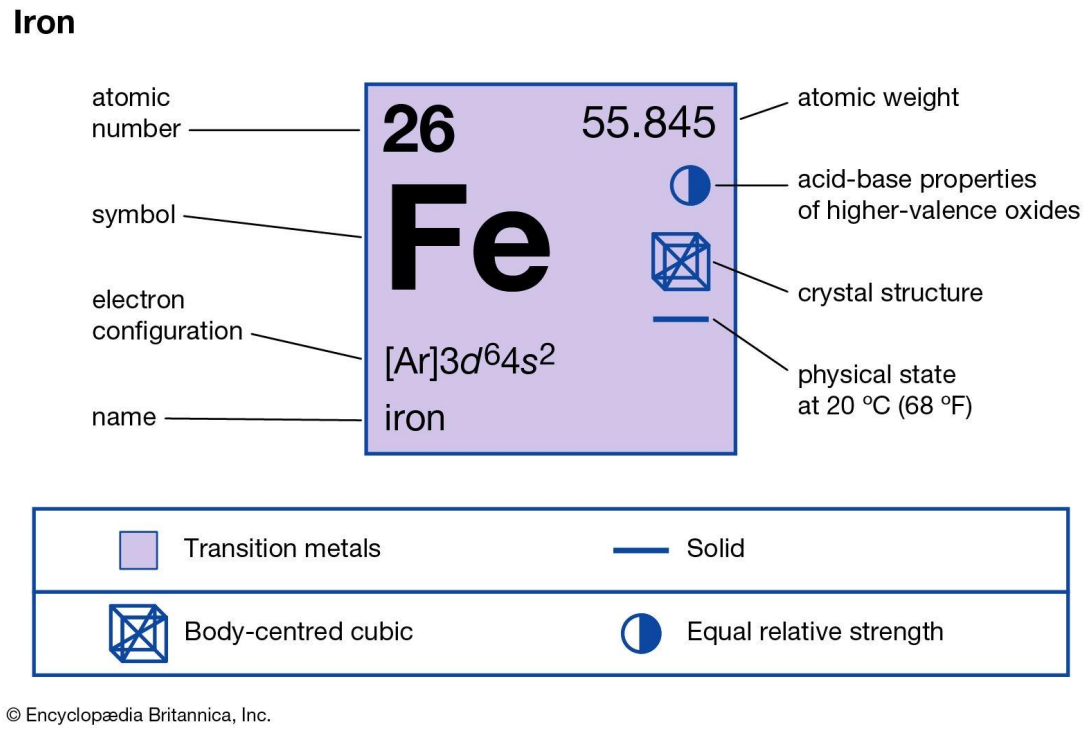

Fig.1.1 properties of iron

1.2.2.4 Chemical Properties of Iron (Fe)

Iron is a moderately reactive transition metal that readily participates in redox reactions, reflecting its ability to exist in multiple oxidation states, primarily +2 (ferrous) and +3 (ferric). These states interconvert easily, making iron essential in biological systems but also influencing its environmental chemistry (RSC, 2025).

In the presence of oxygen and moisture, iron undergoes corrosion, forming hydrated ferric oxides (commonly known as rust). The overall reaction involves the oxidation of Fe to Fe^{2+}, which is then further oxidized to Fe^{3+},

combining with hydroxide ions to produce $Fe(OH)_3$, which dehydrates to $Fe_2O_3 \cdot xH_2O$ (Britannica, 2025).

Iron reacts readily with dilute mineral acids such as hydrochloric acid, liberating hydrogen gas:

$$Fe_{(s)} + 2HCl_{(aq)} \rightarrow FeCl_{2(aq)} + H_{2(g)}$$

In oxidizing environments, ferric salts such as $FeCl_3$ can also form, especially in the presence of chlorine or strong oxidizers. However, iron does not dissolve readily in concentrated nitric acid because of passivation by a protective oxide layer (RSC, 2025).

At elevated temperatures, iron combines directly with non-metals. It reacts with oxygen to form oxides such as FeO, Fe_2O_3, and Fe_3O_4, with the specific phase depending on temperature and oxygen partial pressure. Similarly, it reacts with sulfur to form FeS and with halogens to form ferric halides (MFG Shop, 2025).

Iron also forms a wide range of complex compounds with ligands such as cyanide, carbonyl, and ethylenediamine, which are important in industrial and biochemical processes. These coordination complexes reflect iron's role as a versatile transition metal (RSC, 2025).

1.2.2.5 Isotopes of Iron (Fe)

Iron has four stable isotopes: ^{54}Fe, ^{56}Fe, ^{57}Fe, and ^{58}Fe, with ^{56}Fe being the most abundant, accounting for about 91.75% of natural iron. The other stable isotopes occur in smaller proportions: ^{54}Fe (5.8%), ^{57}Fe (2.1%), and ^{58}Fe (0.28%) (RSC, 2025).

Among these, ^{56}Fe is the most common isotope and plays a crucial role in

geochemical and biological processes. Iron isotopes are widely used in environmental and planetary sciences for tracing geochemical pathways, biogeochemical cycling, and processes such as mineral formation (Craddock *et al.,* 2013).

In addition to the stable isotopes, iron has several radioactive isotopes, the most notable being ^{59}Fe, with a half-life of approximately 44.5 days, used as a tracer in medical and biological research to study iron metabolism (IAEA, 2024). Another significant radioisotope is ^{60}Fe, with a much longer half-life of 2.6 million years, found in cosmic dust and important in astrophysical studies of stellar nucleosynthesis (Wallner *et al.,* 2016).

The natural isotopic composition of iron and its fractionation patterns provide valuable insights into environmental processes, such as weathering, ore formation, and nutrient cycling, making isotopic analysis a useful tool in geochemistry and environmental science (Craddock *et al.,* 2013)

Table 1.2.2.5: Isotopes of Iron (Fe), Abundance, and Half-life

Isotope	Type Natural Abundance (%)	Half-life	Notes
^{54}FeStable	~5.8	Stable	Minor stable isotope
^{56}FeStable	~91.75	Stable	Most abundant isotope
^{57}FeStable	~2.12	Stable	Used in Mössbauer spectroscopy

^{58}FeStable	~0.28	Stable	List abundant stable isotope
^{59}FeRadioactive	Trace (synthetic)	44.5 days	Used in biological trace studies
^{60}FeRadioactive	Extinct radionuclide (cosmic origin)	~2.6 million years	Important in astrophysics, supernova evidence.

1.2.2.6 Characteristics of Iron (Fe)

Iron (Fe) is one of the most abundant transition metals, making up about 5% of the Earth's crust and forming a major part of the planet's core (RSC, 2025). It commonly occurs in ores such as hematite (Fe_2O_3) and magnetite (Fe_3O_4).

It is chemically versatile due to its ability to exist in multiple oxidation states, mainly Fe^{2+} and Fe^{3+}, which play key roles in redox reactions, mineral cycles, and biological processes (Britannica, 2025). This same property also makes it prone to corrosion, forming rust in the presence of air and moisture.

Iron is strongly ferromagnetic below its Curie point of approximately 770 °C, a characteristic that influences both its natural occurrence in magnetic minerals and its technological use (Krebs *et al.,* 2020).

Biologically, it is an essential element required for hemoglobin, enzymes, and energy metabolism, but excess iron is toxic, promoting oxidative stress in organisms (Li *et al.,* 2019).

1.2.2.7 Occurrence and Sources of Iron (Fe)

Iron is the fourth most abundant element in the Earth's crust, constituting about 5% by weight (RSC, 2025). It also forms a major part of the Earth's core, which explains the planet's strong magnetic field. In nature, iron does not occur in its pure metallic form but as oxides, carbonates, and sulfides in various mineral ores. The most common ores are hematite (Fe_2O_3), magnetite (Fe_3O_4), limonite ($FeO(OH)\cdot nH_2O$), and siderite ($FeCO_3$) (Britannica, 2025).

Major geological sources of iron include large ore deposits in regions such as Australia, Brazil, Russia, and China, which dominate global production. In Nigeria, significant iron ore deposits are found in Itakpe (Kogi State) and other parts of the Middle Belt, where mining activities contribute to both economic development and environmental contamination (Onakpa *et al.,* 2018).

Apart from geological ores, iron is also introduced into the environment through anthropogenic activities. Industrial processes such as steel manufacturing, mining, and smelting release iron into soils, air, and water systems. Agricultural practices, including the use of iron-based fertilizers and pesticides, are additional sources. Urban environments also accumulate iron from vehicular emissions, corroded infrastructure, and wastewater discharges (Nkwunonwo *et al.,* 2020).

Biologically, iron is widespread in living systems. It is absorbed by plants from soil in the form of Fe^{2+} and Fe^{3+} ions and incorporated into chlorophyll and enzymatic systems. In animals and humans, dietary iron from plant and animal sources supports hemoglobin synthesis, energy metabolism, and enzyme functions (Li *et al.,* 2019).

Thus, the occurrence and sources of iron span natural geological reservoirs, industrial activities, agricultural inputs, and biological systems, making it both

an essential and environmentally significant element.

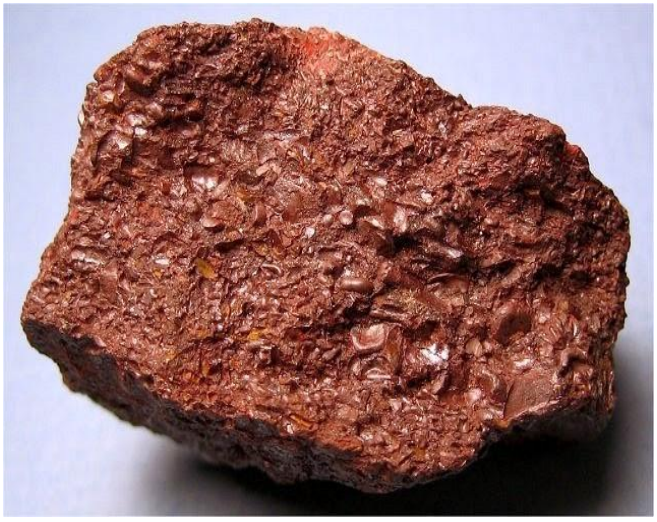

Fig.1.2: iron ore mineral

1.2.2.8 Exposure Routes of Iron (Fe)

Iron, being abundant in nature and widely used in industry, enters biological and environmental systems through multiple exposure routes. The main routes of exposure are ingestion, inhalation, and dermal contact, though the extent of absorption and impact varies with each pathway.

Ingestion is the most common route of iron exposure for humans and animals. Naturally, iron is present in food and drinking water, where it occurs as Fe^{2+} and Fe^{3+} ions. While dietary iron is essential, excessive intake—often from contaminated water supplies or crops grown on polluted soils—can lead to iron overload. This is a particular concern in mining regions and communities near industrial discharges (Onakpa *et al.,* 2018).

Inhalation occurs primarily in occupational settings such as mining, smelting,

and steel production, where airborne iron dust and fumes are common. Prolonged inhalation of iron-rich particulates can lead to siderosis, a type of pneumoconiosis characterized by lung tissue changes due to iron deposition (WHO, 2021). In urban environments, vehicle emissions and industrial air pollution also contribute to inhalable iron particles.

Dermal contact represents a less significant route, as intact human skin does not readily absorb iron. However, repeated contact with iron-containing dust, soil, or wastewater can cause local irritation or contribute to occupational exposure in miners and industrial workers (Nkwunonwo *et al.,* 2020).

In plants, iron is taken up from soil solutions through root systems, especially under reducing conditions where Fe^{2+} is more soluble. Excessive iron uptake in plants, such as in flooded or acidic soils, results in phytotoxicity, leaf bronzing, and stunted growth (Li *et al.,* 2019). Animals and humans are indirectly exposed through consumption of these contaminated plants and water sources, leading to bioaccumulation through the food chain.

Overall, exposure to iron occurs through dietary intake, occupational inhalation, and environmental contact, with ingestion being the primary pathway for the general population, and inhalation the key risk for workers in iron-related industries.

1.2.2.9 Effects of Iron Exposure on the Human Body

Iron is essential for normal physiological functioning, but excessive exposure or accumulation can damage multiple organ systems. The toxic effects of iron vary by age group and severity of exposure**.**

IN CHILDREN

Severe Iron Overload / Acute Poisoning:

- Vomiting and diarrhea (often bloody)
- Metabolic acidosis
- Shock and multi-organ failure
- Hepatic necrosis (liver damage)
- Coma
- Death (Andrews & Schmidt, 2007; WHO, 2020)

Mild to Moderate Iron Overload:

- Abdominal pain and gastrointestinal distress
- Nausea and loss of appetite
- Growth retardation
- Cognitive impairment and learning difficulties
- Behavioral issues linked to oxidative stress
- Increased susceptibility to infections (WHO, 2020; Li *et al.,* 2019)

IN ADULTS

Severe Iron Overload (Chronic / Hemochromatosis):

- Liver cirrhosis and fibrosis
- Diabetes mellitus (due to pancreatic damage)
- Cardiomyopathy and heart failure
- Arthropathy (joint damage)
- Endocrine dysfunction (hypogonadism, pituitary damage)
- Increased risk of hepatocellular carcinoma (Pietrangelo, 2015; Nkwunonwo *et al.,* 2020)

Mild to Moderate Iron Overload:

- Fatigue and weakness
- Abdominal discomfort

- Skin pigmentation (“bronze diabetes”)
- Reduced libido and infertility
- Joint pain
- Depression and mood changes
- Oxidative stress–related symptoms such as dizziness and headaches (WHO, 2021; Andrews & Schmidt, 2007)

1.2.2.10 Systems Affected by Excess Iron (Fe)

Liver (primary site of overload). The liver is the main depot for excess iron, and progressive parenchymal deposition drives oxidative injury, steatohepatitis-like changes, fibrosis, cirrhosis, and at advanced stages elevated hepatocellular carcinoma risk. Early detection and iron removal (e.g., phlebotomy) prevent most hepatic complications, underscoring why the liver is central to iron-toxicity pathways (Zoller *et al.,* 2022; Girelli *et al.,* 2024).

Heart. Myocardial iron accumulation produces diastolic and/or systolic dysfunction, restrictive or dilated cardiomyopathy, and ventricular arrhythmias. Cardiac involvement is a major determinant of prognosis in transfusional and hereditary iron overload, and T2* MRI is pivotal for detection and monitoring (Pennell *et al.,* 2023; Agrawal *et al.,* 2025).

Endocrine (pancreas, pituitary–gonadal axis, thyroid). Iron deposition in pancreatic islets contributes to dysglycemia and diabetes; iron in the pituitary often causes hypogonadotropic hypogonadism (low libido, infertility, amenorrhea), particularly in severe/juvenile forms or long-standing overload. These endocrine toxicities are well-documented clinical manifestations of systemic iron excess (Zoller *et al.,* 2022; Piperno, 2020).

Hematologic/immune regulation. Iron excess and hepcidin dysregulation alter iron trafficking, promoting non-transferrin-bound iron and oxidative stress while also shaping host–pathogen interactions (iron availability favors certain pathogens). Disturbances of the hepcidin–ferroportin axis are central to both overload and anemia-of-inflammation phenotypes (Ganz & Nemeth, 2021; Girelli *et al.,* 2024).

Nervous system. Although the liver and heart are the most clinically affected organs, brain iron dyshomeostasis is implicated in neurodegeneration; excess regional brain iron burdens are linked to oxidative stress and neuronal vulnerability in disorders such as Parkinson's disease. These mechanistic links strengthen the biological plausibility that chronic iron excess can have neurologic consequences (Zecca *et al.,* 2023; Ward *et al.,* 2024).

Respiratory (inhalational iron oxides). Occupational inhalation of iron-rich fumes/dust (e.g., welding) can cause pulmonary siderosis, an iron-laden pneumoconiosis that may present with cough, dyspnea, or asymptomatic radiographic opacities; minimizing airborne exposure is the key preventive measure (Hathaway & Muthusamy, 2023; Saad *et al.,* 2020).

Musculoskeletal & skin. A characteristic, often refractory arthropathy (classically 2nd/3rd MCP joints, ankles, hips) occurs in hereditary hemochromatosis and may persist despite iron removal. Cutaneous hyperpigmentation ("bronzing") reflects increased melanin and dermal iron and often accompanies advanced systemic overload (Calori *et al.,* 2023; Szczerbińska *et al.,* 2024; Zoller *et al.,* 2022).

1.2.2.11 Prevention and Management of Excess Iron (Fe)

Preventing iron overload requires a combination of early detection, medical intervention, and lifestyle adjustments. Because iron cannot be actively

excreted in large amounts by the human body, accumulation over time, whether from genetic causes or environmental exposure can result in organ damage. Preventive strategies therefore focus on limiting intake in at-risk individuals, timely diagnosis, and reducing body iron burden when overload occurs.

General Preventive Measures

Routine screening for individuals with a family history of hereditary hemochromatosis or those undergoing long-term blood transfusions is crucial. Early detection through serum ferritin and transferrin saturation tests allows for intervention before organ injury develops (EASL, 2022). Public awareness campaigns targeting communities near mining and smelting industries can also reduce environmental exposure risks (WHO, 2023).

Medical and Clinical Management

The cornerstone of treatment for hereditary or primary iron overload is therapeutic phlebotomy, a procedure in which blood is periodically removed to lower body iron stores. For patients unable to undergo phlebotomy, such as those with anemia or poor venous access**,** iron chelation therapy using agents like deferoxamine, deferasirox, or deferiprone is recommended (Camaschella, 2019; Girelli *et al.,* 2024). Monitoring with MRI (e.g., T2* imaging) guides treatment effectiveness, especially for cardiac and hepatic iron overload (Pennell *et al.,* 2023).

Lifestyle and Nutritional Strategies

At-risk individuals are often advised to avoid iron supplements, limit red meat and iron-fortified foods, and reduce alcohol consumption, as alcohol exacerbates hepatic iron deposition and injury (Mayo Clinic, 2025). Vitamin C supplementation should also be moderated because it enhances dietary iron

absorption, potentially worsening overload (NIH, 2024). Conversely, regular blood donation in non-anemic individuals may serve as a simple preventive tool for lowering iron stores.

Community and Occupational Interventions

In industrial and mining regions, measures such as dust suppression, improved ventilation, protective masks, and periodic health checks for workers reduce inhalational exposure to iron oxides (Hathaway & Muthusamy, 2023). Environmental regulations that limit industrial effluents into soil and water are equally important in preventing chronic community exposure.

1.2.2.12 Applications of Iron

Iron is one of the most widely used metals in human civilization, serving as the backbone of modern industry, construction, and technology. Its versatility arises from its abundance, mechanical strength, and ability to form alloys such as steel, which revolutionized infrastructure and manufacturing. Beyond structural uses, iron also plays key roles in chemistry, energy, and biological systems.

Industrial and Construction Applications

The majority of extracted iron is converted into steel, an alloy of iron and carbon that dominates the global construction, transport, and machinery sectors. Steel's strength, ductility, and recyclability make it indispensable for building bridges, skyscrapers, pipelines, and transportation systems (World Steel Association, 2023). The automobile and shipbuilding industries also rely heavily on iron and its alloys for structural frames, engines, and reinforcement (Britannica, 2025).

Mechanical and Manufacturing Uses

Iron's magnetic properties and machinability make it a key material in machinery and tool manufacturing. Cast iron, for example, is used in engine blocks, pipes, and machine parts, while wrought iron, though less common today, has historically been valued for ornamental work and corrosion resistance (RSC, 2025). In heavy industries, iron-based alloys serve in turbine components, railways, and industrial plants where durability under stress is essential.

Chemical and Catalytic Roles

In addition to structural uses, iron compounds find application in the chemical industry. Iron oxides serve as catalysts in Haber–Bosch ammonia synthesis and Fischer–Tropsch hydrocarbon production (Smith *et al.,* 2021). Iron salts such as ferric chloride are widely used in water treatment for coagulation and removal of impurities, while iron sulfate is applied in pigments, dyes, and as a soil conditioner in agriculture (Gupta & Gupta, 2022).

Biomedical and Nutritional Uses

Iron's biological importance has also led to applications in medicine and nutrition. Ferrous and ferric salts are incorporated into supplements to treat iron-deficiency anemia, one of the most widespread micronutrient deficiencies globally (WHO, 2023). Moreover, iron oxides are utilized in magnetic resonance imaging (MRI) as contrast agents and in targeted drug delivery systems due to their superparamagnetic properties (Huang *et al.,* 2022).

Energy and Environmental Applications

Iron plays a growing role in sustainable energy systems. Iron-based materials are being investigated for battery electrodes, including emerging rechargeable iron–air and lithium–iron–phosphate batteries (Goodenough & Park, 2013). In environmental remediation, nanoscale zero-valent iron (nZVI) is employed for groundwater decontamination, reducing chlorinated hydrocarbons and immobilizing heavy metals (Yan *et al.,* 2021).

1.2.3 Clay Minerals and Their Characteristic Properties

The recognition of clay as a distinct geological material dates back to the early foundations of geology. Georgius Agricola (1494–1555), widely regarded as the father of mineralogy, provided one of the first recorded definitions of clay in 1546. Since then, the concept of clay has undergone significant refinement, reflecting advances in mineralogical science. The most widely accepted definition today is that proposed by the Joint Nomenclature Committees (JNCs) of the Association Internationale pour l'Étude des Argiles (AIPEA) and the Clay Minerals Society (CMS). They define clay as a naturally occurring material composed primarily of fine-grained minerals that exhibit plasticity upon the addition of water and that harden upon drying or firing. This definition distinguishes natural clays from engineered or synthetic clay-like substances, which may share some properties but differ in origin (Kumari *et al.,* 2021).

Clay minerals occupy a unique position at the Earth's surface, forming at the critical interface between the lithosphere, hydrosphere, and atmosphere. Structurally, they are phyllosilicates composed mainly of silicon–oxygen tetrahedra and aluminum–oxygen or magnesium–oxygen octahedra, often with substitutions involving iron, potassium, sodium, calcium, and other cations (Liu *et al.,* 2022). Their formation requires the presence of water, and as such,

they are common products of weathering, hydrothermal alteration, and sedimentary processes.

Beyond their geological significance, clays have played an essential role in human civilization since antiquity. They have been used for pottery, construction, and agriculture, while in modern contexts they are applied in adsorption, catalysis, pharmaceuticals, cosmetics, and environmental remediation (Britannica, 2025). From a scientific perspective, clays have also been implicated in abiogenesis theories, where their layered structures may have provided catalytic surfaces for the assembly of organic molecules critical to the origin of life (Liu *et al.,* 2022).

1.2.3.1 Classification of Clay Minerals

Clay minerals are classified principally by the way their basic sheets — silica tetrahedral (T) sheets and alumina/magnesia octahedral (O) sheets are stacked. That stacking (and the chemistry within the sheets) controls layer spacing, interlayer chemistry, surface charge and therefore the physical and chemical behaviour of the clay (e.g., swelling, cation-exchange capacity). Modern practical and regulatory descriptions of clay likewise emphasise particle size, plasticity when wet, and hardening on drying/firing as defining features of "clay" products (Clay Minerals Society, 2020; Damato *et al.,* 2022).

1:1 clays (TO structure) — In this group each structural unit (layer) contains one tetrahedral sheet bonded to one octahedral sheet. Typical minerals are kaolinite, dickite, nacrite and halloysite. The TO layer is held to the next layer by strong hydrogen bonding, so these clays have limited interlayer space**,** low swelling**,** low surface area and relatively low cation-exchange capacity (CEC). Because of their stability and low reactivity, 1:1 clays are widely used in

ceramics, paper fillers and some pharmaceutical applications (Damato *et al.,* 2022).

2:1 clays (TOT structure) — These layers have an octahedral sheet sandwiched between two tetrahedral sheets. Prominent examples are the smectite group (montmorillonite/bentonite), vermiculite and illite (illite is 2:1 but non-expanding — see below). In expandable 2:1 clays (smectites), weak interlayer forces and the presence of exchangeable cations allow water and ions to enter the interlayer space, producing high swelling capacity**,** large specific surface area**,** and high CEC. Those properties make smectites particularly effective adsorbents for metal ions and useful in remediation, sealants and drilling muds (Soltaninejad *et al.,* 2023; Damato *et al.,* 2022).

2:1:1 clays (TOT + brucite layer) — Chlorite and chlorite-like minerals contain the 2:1 layer plus an additional brucite-like (hydroxide) octahedral sheet in the interlayer. The extra sheet strengthens interlayer bonding and yields a more stable, less expandable structure than smectites; chlorites are therefore less prone to swelling and generally show lower CEC than expandable 2:1 clays (Clay Minerals Society, 2020).

Other categories: mixed-layer and fibrous clays — Natural clays are often more complicated than a single ideal type. Mixed-layer (interstratified) clays (e.g., illite–smectite, kaolinite–smectite) contain alternating or irregular sequences of 1:1 and 2:1 layers and therefore display intermediate behaviour. Fibrous clays (palygorskite, sepiolite) have chain-like structures rather than platey sheets; they provide high surface area and distinct adsorption sites useful in specialized adsorbent and catalytic roles (Damato *et al.,* 2022).

A key chemical control across these groups is isomorphic substitution (e.g., Al^{3+} for Si^{4+} in tetrahedral sites or Mg^{2+}/Fe^{2+} for Al^{3+} in octahedral sites), which creates a permanent negative layer charge balanced by exchangeable

cations (Na^{+}, Ca^{2+}, K^{+}). That permanent charge underlies the cation-exchange behaviour central to heavy-metal adsorption and is the reason 2:1 expandable clays (smectites/bentonites) are often the most effective natural adsorbents in remediation studies (Damato *et al.,* 2022; Soltaninejad *et al.,* 2023).

.

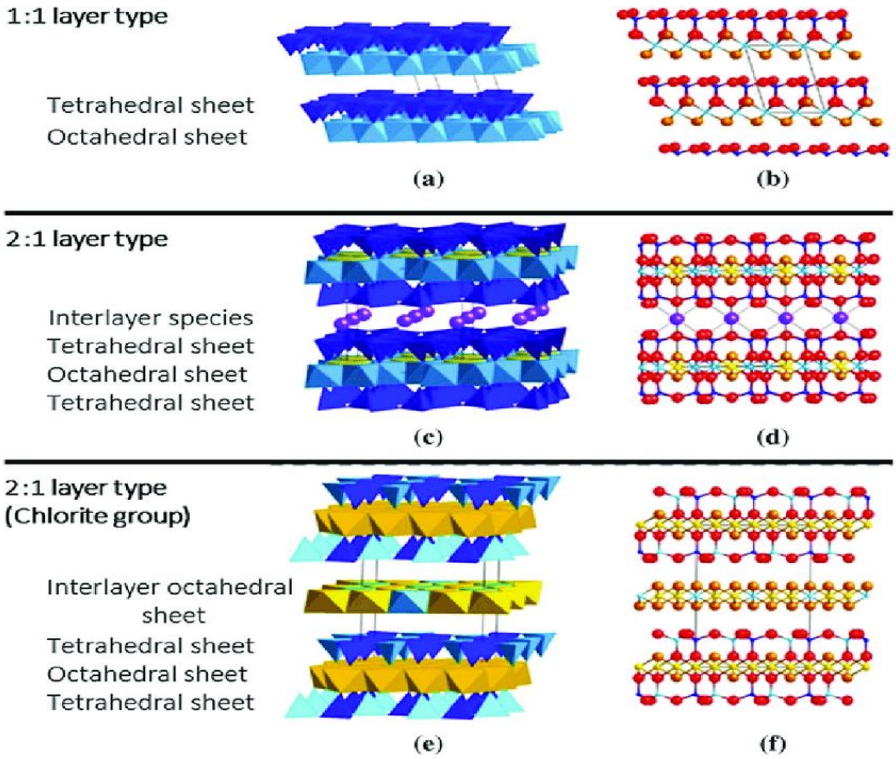

Fig. 1.3 clay classifications

1.2.3.2 Characteristic Properties of Clay Minerals

Clay minerals exhibit a set of characteristic physical and chemical properties that distinguish them from other soil constituents and determine their effectiveness as adsorbents. These properties arise from their layered phyllosilicate structure, surface chemistry, and ion-exchange capacity. A clear

understanding of these features is crucial in evaluating their suitability for applications such as heavy metal adsorption, environmental remediation, and industrial use (Kumari *et al.,* 2021; Gu *et al.,* 2019).

1. Surface area and porosity

Clay minerals possess high specific surface areas, ranging from ~10 m^2/g in kaolinite to more than 800 m^2/g in smectites and sepiolite. Their layered or fibrous morphology provides abundant active sites for adsorption, while interlayer regions and micropores enhance their capacity to trap ions and molecules (Gu *et al.,* 2019).

2. Cation exchange capacity (CEC)

CEC refers to the ability of clays to exchange cations between their surfaces/interlayers and the surrounding solution. It arises mainly from isomorphic substitution (e.g., Mg^{2+} replacing Al^{3+} in octahedral sites), which imparts a permanent negative charge. Smectites typically have the highest CEC (80–150 meq/100g), while kaolinite has the lowest (3–15 meq/100g) (Soltaninejad *et al.,* 2023).

3. Plasticity and swelling behavior

When mixed with water, clay minerals exhibit plasticity, enabling them to be molded and shaped. 2:1 clays such as montmorillonite swell extensively due to interlayer expansion, whereas 1:1 clays like kaolinite remain dimensionally stable. This swelling property enhances the adsorption of water and solutes but can also limit their geotechnical stability (Damato *et al.,* 2022).

4. Surface charge and functional groups

Clay mineral surfaces contain hydroxyl (–OH), silanol (Si–OH), and aluminol (Al–OH) groups. These functional groups, combined with the layer charge from isomorphic substitution, create reactive sites for ion exchange, hydrogen bonding, and surface complexation with heavy metals. Surface charge is

pH-dependent: at low pH, competition with protons reduces metal adsorption, whereas at higher pH, increased deprotonation enhances binding capacity (Kumari *et al.,* 2021).

5. Thermal and chemical stability

Clays are generally stable under moderate thermal and chemical conditions, but extreme environments alter their structure. Heating beyond 500 °C dehydroxylates clays, destroying their crystalline order, while acid activation leaches structural cations and increases surface area. These modifications can enhance adsorption performance but may reduce stability in long-term use (Gu *et al.,* 2019).

6. Sorption selectivity

Different clays show variable affinity for specific metal ions, depending on ion size, hydration energy, and layer charge density. For example, montmorillonite has strong affinity for Pb^{2+}, Cu^{2+}, and Fe^{3+}, while kaolinite exhibits weaker but still useful sorption. This selectivity is important in designing remediation strategies for targeted contaminants (Soltaninejad *et al.,* 2023).

The characteristic properties of clay minerals—high surface area, cation exchange capacity, swelling, surface reactivity, and structural modifiability—make them versatile materials for environmental remediation. These properties explain their increasing use as natural adsorbents in the removal of heavy metals such as iron from contaminated systems.

1.2.3.3 Advantages of Clay over Other Adsorbents

In the search for efficient materials for heavy metal remediation, a wide range of adsorbents has been explored, including activated carbon, zeolites, biochar,

synthetic polymers, and nanomaterials. While each class of material has demonstrated success under specific conditions, clay minerals hold several unique advantages that make them particularly suitable for large-scale, low-cost, and sustainable environmental applications.

1. Abundance and availability

Clays are among the most abundant natural minerals on Earth, occurring widely in soils, riverbeds, and sedimentary deposits. Their widespread availability, particularly in regions such as Nigeria, makes them an easily accessible raw material for remediation without reliance on expensive imports (Kumari *et al.,* 2021).

2. Low cost

Unlike activated carbon or engineered nanomaterials, which require high production costs and sophisticated processing, clays can often be used in their natural or minimally processed forms. Even when modification is performed (e.g., acid activation), the associated costs are still lower than for synthetic adsorbents (Gu *et al.,* 2019).

3. High surface area and cation exchange capacity (CEC)

Smectites and other 2:1 clays exhibit high surface areas and large CEC, comparable to or exceeding that of many synthetic resins and zeolites. These structural features provide numerous active sites for heavy metal ion adsorption, enhancing their effectiveness even at low adsorbent dosages (Soltaninejad *et al.,* 2023).

4. Versatility and modifiability

Clays can be easily modified to improve performance, for example, by acid treatment to increase porosity, pillaring to stabilize interlayer spacing, or organic modification to increase affinity for hydrophobic contaminants. This

versatility allows clays to compete with advanced engineered adsorbents while remaining cost-effective (Gu *et al.,* 2019; Wang *et al.,* 2024).

5. Environmental friendliness

Clays are non-toxic, naturally occurring materials that generally pose minimal ecological risks compared to synthetic polymers or nanomaterials, which may introduce secondary pollution. Their safe handling and disposal reduce the environmental footprint of remediation projects (Damato *et al.,* 2022).

6. Local adaptability

Because clays are geologically diverse, their composition and properties vary by location. This allows researchers to identify and utilize local clays, such as Aseni clay in Kogi State, Nigeria, which may offer unique mineralogical advantages for site-specific environmental cleanup. This local adaptability is an advantage over imported adsorbents that may not be optimized for regional conditions (Achievers University Report, 2023).

1.2.4 Atomic Absorption Spectroscopy (AAS)

Atomic Absorption Spectroscopy (AAS) is a quantitative analytical method used to determine metal concentrations in samples such as soil, water, plants, and biological tissues. The technique relies on the ability of ground-state atoms to absorb light of a specific wavelength, with the degree of absorption directly related to the concentration of the metal present (Yang, 2024).

Developed by Alan Walsh in the 1950s, AAS has become a standard method for trace metal analysis because of its accuracy, sensitivity, and relatively low cost compared to advanced techniques like ICP-OES or ICP-MS (Bacon *et al.,* 2021). It is particularly valuable in environmental studies for monitoring heavy metals such as Fe, Pb, Cd, and As (Tibebe *et al.,* 2022).

Despite newer methods, AAS remains widely used due to its affordability, simplicity, and reliability, making it especially suitable for laboratories in developing regions. For iron analysis, AAS provides reproducible and precise measurements, supporting studies such as this one, which investigates the adsorption of Fe using Aseni clay (Negrão *et al.,* 2023).

1.2.4.1 Instrumentation of AAS

The instrumentation of Atomic Absorption Spectroscopy (AAS) is designed to generate free atoms, expose them to a light source at specific wavelengths, and measure the degree of light absorption. The main components include:

1. **Radiation Source**

   Usually a hollow cathode lamp (HCL) specific to the element of interest. For Fe analysis, an iron cathode lamp emits the characteristic wavelength absorbed by Fe atoms (Bacon *et al.,* 2021).
2. **Atomizer**

   Converts the sample into free atoms. Two types are common:
   - **Flame atomizer**: Sample solution is nebulized into a flame (air–acetylene or nitrous oxide–acetylene), creating ground-state atoms.
   - **Graphite furnace atomizer (electrothermal AAS)**: Provides higher sensitivity by heating samples in a graphite tube to produce atoms without a flame (Tibebe *et al.,* 2022).
3. **Monochromator**

   Isolates the specific wavelength of interest from the lamp, ensuring only the radiation absorbed by the analyte (e.g., Fe at 248.3 nm) is measured (Yang, 2024).
4. **Detector**

   A photomultiplier tube (PMT) or solid-state detector measures the

intensity of transmitted light, which decreases in proportion to the number of atoms absorbing it (Negrão *et al.,* 2023).

5. **Readout System**

   Converts the detector signal into absorbance values displayed digitally. These values are compared to calibration curves prepared from standard solutions to determine metal concentrations.

1.2.5 Adsorption

Adsorption is a surface process in which molecules, ions, or atoms from a fluid phase accumulate on the surface of a solid or liquid. Unlike absorption, which occurs throughout the bulk of a material, adsorption is restricted to the surface (Foo & Hameed, 2019).

The process is mainly divided into physisorption, governed by weak van der Waals forces and reversible in nature, and chemisorption, which involves stronger chemical bonds and higher specificity (Wang *et al.,* 2023).

In environmental remediation, adsorption is considered one of the most effective and low-cost methods for removing pollutants, particularly heavy metals, from contaminated systems. Clay minerals are among the most widely used adsorbents due to their layered structure, high surface area, and cation-exchange capacity, making them highly suitable for trapping ions such as Fe^{3+} (Kumari *et al.,* 2021).

The efficiency of adsorption is commonly studied through isotherm models (e.g., Langmuir and Freundlich) and kinetic models (e.g., pseudo-first- and second-order), which help explain the capacity, mechanisms, and rates of adsorption (Mokarram *et al.,* 2022).

1.2.5.1 Types of Adsorption

Adsorption processes are generally classified into two main types: physisorption and chemisorption. The distinction lies in the nature of the forces that hold the adsorbate on the adsorbent surface.

1. Physisorption (Physical Adsorption)

Physisorption occurs when the adsorbate molecules are bound to the surface by weak van der Waals forces. It is typically reversible and does not involve any significant electron transfer or chemical reaction.

- It takes place at relatively low temperatures and decreases with increasing temperature.
- Adsorption energy is low (usually <40 kJ/mol).
- Multiple layers of adsorbate molecules may form on the surface.
- It is less specific, meaning many types of molecules can be adsorbed on the same surface (Singh *et al.,* 2021).

2. Chemisorption (Chemical Adsorption)

Chemisorption involves the formation of stronger chemical bonds (ionic or covalent) between adsorbate and adsorbent surface sites.

- It usually occurs at higher temperatures compared to physisorption.
- Adsorption energy is higher (40–800 kJ/mol).
- Typically results in monolayer adsorption.
- It is highly specific, depending on the chemical reactivity of the adsorbent surface (Wang *et al.,* 2023).

In many environmental applications, both physisorption and chemisorption may occur simultaneously. For instance, clays can first trap metal ions electrostatically (physisorption) and later bind them more strongly through ion exchange or surface complexation (chemisorption). This duality enhances their overall adsorption efficiency (Kumari *et al.,* 2021).

1.2.5.2 Factors Affecting Adsorption

The efficiency and extent of adsorption depend on several factors related to the adsorbent, adsorbate, and experimental conditions. Key factors include:

1. Surface Area of Adsorbent

The greater the surface area of the adsorbent, the higher its adsorption capacity. Materials with fine particle size (e.g., clays, activated carbon) offer more active sites for interaction with metal ions (Wang *et al.,* 2023).

2. Nature of the Adsorbent

Chemical composition, pore size, surface functional groups, and cation exchange capacity strongly influence adsorption performance. For clays, the presence of –OH groups, silica-alumina layers, and isomorphic substitutions enhance the binding of cations such as Fe^{3+} (Kumari *et al.,* 2021).

3. Nature and Concentration of Adsorbate

Higher concentrations of metal ions increase the driving force for mass transfer, enhancing adsorption until saturation is reached. The ionic radius, charge density, and hydration energy of the adsorbate also play critical roles. For example, trivalent Fe^{3+} ions exhibit stronger adsorption than monovalent ions due to higher charge density (Mokarram *et al.,* 2022).

4. pH of the Medium

pH affects both the surface charge of the adsorbent and the speciation of the adsorbate. At low pH, excess H^+ ions compete with metal cations for adsorption sites, reducing uptake. Optimal adsorption often occurs at neutral to slightly alkaline conditions, although precipitation of $Fe(OH)_3$ may occur at very high pH (Bhatnagar & Sillanpää, 2022).

5. Temperature

Temperature influences adsorption capacity depending on whether the process is exothermic or endothermic. Physisorption generally decreases with temperature rise, while chemisorption may increase due to enhanced activation energy.

6. Contact Time

Adsorption increases with contact time until equilibrium is reached. The rate is controlled by diffusion of ions into pores and availability of active sites.

7. Presence of Competing Ions

In real systems, multiple ions may compete for the same adsorption sites, reducing selectivity and efficiency. For example, in wastewater, ions such as Ca^{2+} or Mg^{2+} may compete with Fe^{3+} (Singh *et al.,* 2021).

1.2.5.3 Adsorption Isotherms

Adsorption isotherms describe the relationship between the amount of adsorbate retained on the surface of an adsorbent and its equilibrium concentration in solution at constant temperature. These models are essential for understanding adsorption mechanisms, surface properties, and maximum adsorption capacity (Ayawei *et al.,* 2020; Tran *et al.,* 2021). The most widely applied isotherm models in environmental adsorption studies include:

1. Langmuir Isotherm

Proposed by Irving Langmuir in 1918, this model assumes monolayer adsorption on a homogeneous surface with a finite number of identical binding sites. It implies no interaction between adsorbed molecules. The Langmuir equation is expressed as:

$$q_e = \frac{q_{max} K_L C_e}{1 + K_L C_e}$$

Where:

- qe = amount adsorbed at equilibrium (mg/g)
- Ce = equilibrium concentration of adsorbate (mg/L)
- qmax = maximum adsorption capacity (mg/g)
- KL = Langmuir constant related to affinity (L/mg)

This model is particularly useful in estimating adsorption capacity of clay for Fe^{3+} ions (Tran *et al.,* 2021).

2. Freundlich Isotherm

An empirical model that describes multilayer adsorption on heterogeneous surfaces. It is expressed as:

$$qe = K_F Ce^{1/n}$$

Where:

- K_F = adsorption capacity constant
- 1/n = heterogeneity factor (0 < 1/n < 1 indicates favorable adsorption).

Freundlich is widely applied for natural adsorbents like clay, which often exhibit surface heterogeneity (Ayawei *et al.,* 2020).

1.2.6 Adsorption kinetics

Adsorption kinetics describe the rate and mechanism by which adsorbate species are transferred from the bulk solution to the adsorbent surface and subsequently distributed among available sites. Kinetic analysis is essential for

reactor design and for distinguishing rate-controlling steps such as film diffusion, intraparticle diffusion, and surface chemical reaction. Empirical and semi-empirical kinetic expressions are commonly applied to batch adsorption data to extract rate constants and to suggest dominant mechanisms; however, careful use of linearization and error analysis is necessary because fitting method choice can bias parameter estimates.

1.2.6.1 Pseudo-first-order kinetics

The pseudo-first-order (PFO) model — originally proposed by Lagergren — assumes that the adsorption rate is proportional to the difference between the equilibrium adsorption capacity and the adsorption capacity at any time t. The differential form of the model is expressed as:

$$\frac{dq_t}{dt} = k_1(q_e - q_t)$$

Integrating this expression between the limits $q_t = 0$ at $t = 0$ and $q_t = q_t$ at $t = t$gives the linearized form:

$$\ln (q_e - q_t) = \ln q_e - k_1 t$$

where q_t and q_e (mg·g^{-1}) are the adsorption capacities at time t and at equilibrium respectively, and k_1(min^{-1}) is the pseudo-first-order rate constant. This model generally provides a good fit for systems governed by physisorption or where external mass transfer dominates the rate of uptake. However, it can yield inaccurate kinetic parameters if the equilibrium adsorption capacity q_e is not experimentally determined or if only linear regression is used for fitting. Therefore, comparison between linear and

nonlinear fitting methods with appropriate error analyses is recommended for reliable interpretation.

1.2.6.2 Pseudo-second-order kinetics

The pseudo-second-order (PSO) model assumes that the adsorption rate is proportional to the square of the difference between equilibrium adsorption capacity and adsorption capacity at time t. The differential form of the model is given as:

$$\frac{dq_t}{dt} = k_2(q_e - q_t)^2$$

Integration of this equation with the same boundary conditions yields the linearized form:

$$\frac{t}{q_t} = \frac{1}{k_2 q_e^2} + \frac{t}{q_e}$$

where k_2 (g·mg^{-1}·min^{-1}) is the pseudo-second-order rate constant. The PSO model often provides excellent fits to adsorption data for heavy metals on natural and modified adsorbents and is commonly associated with chemisorption processes involving valence forces through sharing or exchange of electrons. Nevertheless, a good fit with the PSO model alone does not confirm a chemical mechanism; additional supporting evidence such as spectroscopic analysis, activation energy measurements, or surface characterization is required to validate the mechanism. Recent reviews emphasize both the utility of the PSO model for modeling adsorption kinetics and the caution needed in its mechanistic interpretation.

CHAPTER TWO

2.0 MATERIALS AND METHODS

This chapter outlines the materials, reagents, equipment, and experimental procedures employed in assessing the adsorption potential of Aseni clay (second layer)s for the removal of Fe^{3+} ions from aqueous solutions. The methodology was designed to ensure accuracy, reproducibility, and reliability of results while adhering to established scientific protocols for adsorption studies. The work involved sample collection and preparation, physicochemical and spectroscopic characterization of the adsorbent, preparation of Fe^{3+} solutions, and systematic batch adsorption experiments conducted under controlled laboratory conditions. Analytical techniques such as Atomic Absorption Spectroscopy (AAS) were applied to quantify residual metal ion concentrations, while Fourier Transform Infrared Spectroscopy (FTIR) was utilized to evaluate surface functional groups and adsorption-related changes in the clay material.

2.1 MATERIALS

2.1.1 REAGENTS AND CHEMICAL USED

- **Iron(III) chloride hexahydrate ($FeCl_3.6H_2O$)**
- **Clay Sample**
- **Sodium hydroxide**
- **Nitric acid**
- **Distilled Water**

- **Buffers**
- **Hydrochloric acid**

2.1.2 INSTRUMENT AND APPARATUS USED

- **Mortar& Pestle**
- **Sieve**
- **Beakers**
- **Conical flasks**
- **Measuring Cylinder**
- **Sample bottles**
- **Analytical balance**
- **Dropper**
- **Volumetric flask**
- **Separating Funnel**
- **Mechanical Shaker**
- **Filter paper**
- **Spatula**
- **pH metre**
- **Fume Cupboard**
- **Atomic Absorption spectroscopy**
- **Fourier transform infrared spectroscopy**
- **Thermometer**

2.2 METHODS

2.2.1 PREPARATION OF ADSORBENT – Aseni Clay (Second Layer)

Aseni clay (second layer) was collected from Kogi State, Nigeria. Impurities such as stones and roots were removed, and the sample was sun-dried,

followed by oven-drying at 105 °C for 24 h. The dried clay was ground, sieved to <150 μm, and washed repeatedly with distilled water until clear, then re-dried. This process improved surface area and removed soluble impurities. The prepared clay was stored in airtight containers before use. Similar preparation protocols are widely reported for enhancing the adsorption efficiency of natural clays (Akinyeye *et al.,* 2023; Ibrahim *et al.,* 2021; Mansouri *et al.,* 2022).

2.2.2 PREPARATION OF METAL ION SOLUTION(Fe^{3+})

A 1000 mg/L Fe^{3+} stock solution was prepared from Iron(III) chloride hexahydrate ($FeCl_3 \cdot 6H_2O$). Exactly 4.84 g of the precursor was weighed, dissolved in distilled water, and transferred into a 1 L volumetric flask to make up to the mark. The solution was stirred until complete dissolution occurred, ensuring a uniform concentration. This stock was later diluted to desired working concentrations for adsorption experiments. (Hasan *et al.,* 2021).

The choice of $FeCl_3 \cdot 6H_2O$ is common in heavy metal adsorption studies due to its high solubility, stability, and availability as a reliable Fe^{3+} source. Distilled water was used to avoid interference from dissolved ions that could affect adsorption performance (Hasan *et al.,* 2021).

Calculation of 4.84 g $FeCl_3 \cdot 6H_2O$ for 1000 mg/L Fe^{3+} solution

- **Step 1:** Determine molar mass of $FeCl_3 \cdot 6H_2O$
    - Fe = 55.85 g/mol

- Cl3 = 3 × 35.45 = 106.35 g/mol
- $6H_2O$ = 6 × 18.02 = 108.12 g/mol
- Molar mass = 55.85 + 106.35 + 108.12 = 270.32 g/mol

- **Step 2:** Fraction of Fe in $FeCl_3 \cdot 6H_2O$

Mass fraction of Fe = $\frac{55.85}{270.32} = 0.2066$g

Step 3: Mass of $FeCl_3 \cdot 6H_2O$ required to supply 1 g of Fe^{3+}

Required mass = $\frac{1.000}{0.2066}$ = 4.84g

Thus, 4.84 g of $FeCl_3 \cdot 6H_2O$ provides exactly 1 g (1000 mg) of Fe^{3+}, giving a 1000 mg/L Fe^{3+} stock solution.

2.2.3 BATCH ADSORPTION TESTING

Batch adsorption experiments were carried out to investigate the removal efficiency of Fe^{3+} ions by Aseni clay (second layer). The procedure involved preparing 250 mL Erlenmeyer flasks, each containing 100 mL of Fe^{3+} solution at predetermined concentrations. Measured quantities of the clay adsorbent (0.1–1.0 g) were introduced into the flasks, which were then placed on an orbital shaker at 150 rpm to ensure uniform mixing. The influence of adsorbent dosage, initial Fe^{3+} concentration, pH, contact time, and temperature (25–50 °C) was systematically studied under controlled conditions, similar to procedures reported in previous clay adsorption studies (Osobamiro *et al.,* 2020; Abiodun *et al.,* 2023).

After agitation for specified contact times ranging from 10 to 120 minutes, the suspensions were centrifuged at 4000 rpm for 10 minutes, followed by

filtration. The supernatants were analyzed using Atomic Absorption Spectrophotometry (AAS) to determine the residual Fe^{3+} concentration.

The equilibrium adsorption capacity (Q_e, mg/g) and percentage removal (% Removal) were calculated using the following equations, widely applied in adsorption research (Mustapha, 2023):

$$Q_e = \frac{(C_0 - C_e)V}{m}$$

$$\%\, Removal = \frac{(C_0 - C_e)}{C_0} \times 100$$

Where:

- $\mathbf{C_0}$ = initial Fe^{3+} concentration (mg/L)
- $\mathbf{C_e}$ = equilibrium Fe^{3+} concentration (mg/L)
- **V** = volume of solution (L)
- **m** = mass of adsorbent (g)

2.2.3.1 EFFECT OF CONCENTRATION

To investigate the influence of initial Fe^{3+} concentration on adsorption efficiency, batch experiments were conducted using five 250 mL conical flasks, each containing 1.0 g of untreated Aseni clay (second layer) and 100 mL Fe^{3+} solutions of varying concentrations (10, 20, 30, 40, and 50 mg L^{-1}). The suspensions were placed on a mechanical shaker at 150 rpm for 30 minutes at room temperature to ensure uniform mixing and contact between solute and adsorbent. Each concentration condition was performed in triplicate to ensure reproducibility and statistical reliability.

Following agitation, the mixtures were filtered, and the supernatants were collected for analysis. The residual Fe^{3+} concentrations were determined using Atomic Absorption Spectrophotometry (AAS). From these values, adsorption capacity (Q_e) and removal efficiency (%) were calculated.

This method aligns with standard adsorption protocols, where the initial solute concentration serves as a driving force for mass transfer between the aqueous phase and the adsorbent surface. At low concentrations, adsorption sites are readily available, leading to high removal efficiency. As concentration increases, more Fe^{3+} ions compete for active sites, which may eventually lead to surface saturation and reduced efficiency per unit mass of clay (Abiodun *et al.,* 2023; Heliyon, 2023).

2.2.3.2 EFFECT OF ADSORBENT DOSAGE

Batch experiments to evaluate the effect of adsorbent dosage were carried out in 250 mL conical flasks. Five sets of flasks (each condition run in triplicate) were prepared by adding 100 mL of 30 $mg \cdot L^{-1}$ Fe^{3+} solution (from $FeCl_3 \cdot 6H_2O$ stock) to each flask. To each set, measured masses of untreated Aseni clay (2nd layer) — 0.2 g, 0.4 g, 0.6 g, 0.8 g and 1.0 g — were added to give adsorbent dosages of 2.0–10.0 $g \cdot L^{-1}$. The suspensions were agitated on an orbital shaker at ~150 rpm for 30 minutes at ambient laboratory temperature (≈25 ± 2 °C). After agitation, samples were allowed to settle and were filtered to separate the solid phase; the supernatants were collected and the residual Fe concentration measured by Atomic Absorption Spectrophotometry (AAS). Each dose/condition was prepared and analysed in triplicate and the mean ± standard deviation reported. (Moustafa, 2023).

2.2.3.3 EFFECT OF AGITATION TIME

A fixed mass of 1.0 g of untreated Aseni second-layer clay was introduced into 100 mL of 30 $mg \cdot L^{-1}$ $FeCl_3 \cdot 6H_2O$ solution in six conical flasks (all experiments run in triplicate). The flasks were placed on a mechanical shaker operating at a constant speed (~150 rpm) and subjected to different agitation times of 5, 15, 30, 60, 90, and 120 minutes. At each specified interval, suspensions were withdrawn, filtered, and the supernatants analysed using Atomic Absorption Spectroscopy (AAS) to determine residual Fe(III) concentrations.

The adsorption capacity at time t (qt) and percentage removal (%) were calculated from the concentration difference before and after treatment using standard adsorption equations. These time intervals were selected to capture both the rapid initial uptake phase and the approach to equilibrium. Adsorption with natural clays typically exhibits fast removal during the first 15–30 minutes, followed by slower uptake as surface sites become saturated, with equilibrium generally reached within 60–120 minutes (Moustafa, 2023; Sen, 2023).

2.2.3.4 EFFECT OF PH

The effect of solution pH on Fe(III) adsorption by Aseni clay (2nd layer) was investigated using 6 sets of experiments (pH 4, 5, 6, 7, 8 and 9). In each test, 1.0 g of the untreated Aseni clay was added to 100 mL of 30 $mg \cdot L^{-1}$ Fe^{3+} solution (from the $FeCl_3 \cdot 6H_2O$ stock). The pH of each aliquot was carefully adjusted to the target value using dilute 0.1 M HCl or 0.1 M NaOH and verified with a calibrated pH meter before adding the adsorbent. All flasks

were agitated on a mechanical shaker at ~150 rpm for 30 minutes at room temperature; every pH condition was run in triplicate to ensure reproducibility. After agitation, samples were filtered (or centrifuged), and the residual Fe(III) concentration in each filtrate was measured by AAS. Adsorption capacity at equilibrium (Q_e) and percent removal (%) were computed from the measured concentrations. (Middea *et al.,* 2024; Furcas *et al.,* 2024).

CHAPTER THREE

3.0 RESULTS AND DISCUSSION

The tables below were produced from results obtained from Atomic Adsorption Spectrophotometric analysis carried out on the various filtrates obtained from the experiment using Aseni clay(second layer) in heavy metals solutions.

All the equilibrium concentration are calculated from the triplicate values obtained from Atomic Adsorption Spectroscopy (AAS)

3.1 RESULTS

3.1.0 TABLE 3.1: EFFECT OF CONCENTRATION ON ADSORPTION OF Fe^{3+} ION

S/N	INITIAL CONC(mg/L)	EQUILIBRIUM CONC(mg/L)	AMOUNT ADSORBED (mg/L) ± SD	ADSORPTION CAPACITY (qe)	PERCENTAGE ADSORPTION (%)
1	10	0.43	9.57±0.21	0.96	95.70
2	20	1.70	18.30±0.20	1.83	91.50

3	30	4.57	25.43±0.42	2.54	84.77
4	40	10.17	29.83±0.35	2.98	74.57
5	50	13.8	36.20±1.75	3.62	72.40

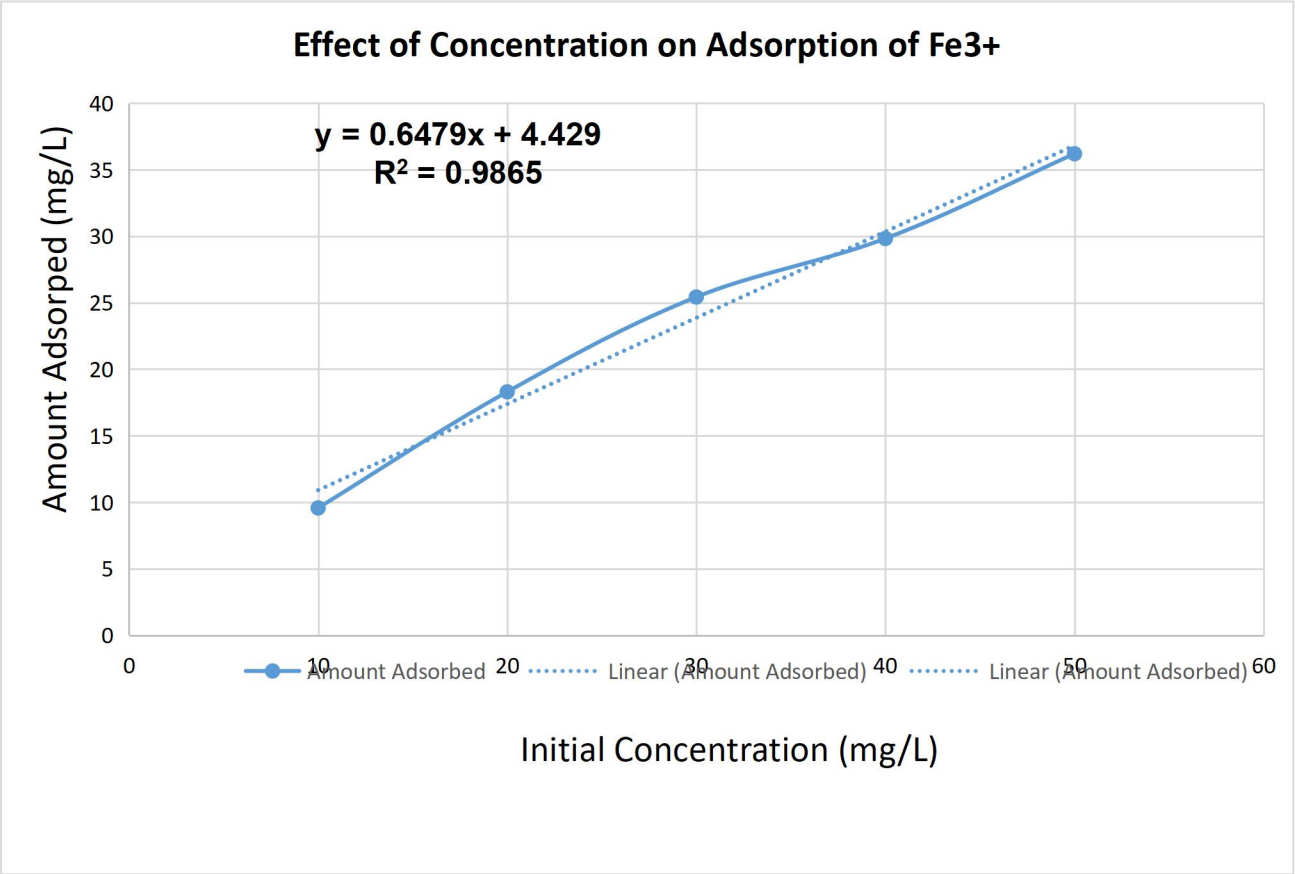

Fig 3.1: Effect of Concentration on Adsorption of Fe^{3+} ion

DISCUSSION: EFFECT OF CONCENTRATION

The adsorption data (Table 1) show that increasing the initial Fe^{3+} concentration from 10 to 50 $mg \cdot L^{-1}$ raised the equilibrium adsorption capacity (q_e) from 0.96 to 3.62 $mg \cdot g^{-1}$ while the percentage removal fell from 95.7% to 72.4%. This response is typical for a fixed mass of adsorbent: lower initial concentrations permit most dissolved ions to occupy abundant surface sites, producing high removal percentages, whereas higher concentrations

increase the mass-transfer driving force and therefore the uptake per gram (q_e) but also push the adsorbent toward surface saturation, reducing the fraction removed. Similar concentration-dependent trends have been observed for natural clay-type adsorbents and palygorskite materials. (Middea *et al.,* 2024; Maged *et al.,* 2023).

Mechanistically, the pattern reflects a balance between enhanced driving force for transfer at higher C_0 and the finite number of adsorption sites (plus possible intra-particle diffusion limitations) that cause percent removal to drop as sites fill. Recent experimental and modeling studies on clay mineral surfaces emphasize how site heterogeneity and diffusion resistance produce the exact behaviour seen here (Orucoglu *et al.,* 2022). Practically, Aseni clay demonstrates useful uptake at low-to-moderate Fe concentrations—suitable for low-cost polishing or pre-treatment—while chemical or thermal activation would be the standard route to increase capacity if higher removal is required (Maged *et al.,* 2023).

3.1.1 TABLE 3.2: EFFECT OF ADSORBENT DOSAGE ON ADSORPTION OF Fe^{3+}ION

S/N	ADSORBENT DOSAGE(g)	INITIAL CONC (mg/L)	EQUILIBRIUM CONC(mg/L)	AMOUNT ADSORBED (mg/L)	ADSORPTION CAPACITY (qe)	PERCENTAGE ADSORPTION (%)
1	0.2	30	12.70	17.30 $\pm$0.17	1.73	57.67
2	0.4	30	8.10	21.90 $\pm$1.00	2.19	73.00
3	0.6	30	6.97	23.03	2.30	76.77

				±0.15		
4	0.8	30	6.50	23.50 ±0.36	2.35	78.33
5	1.0	30	5.03	24.97 ±0.15	2.45	83.23

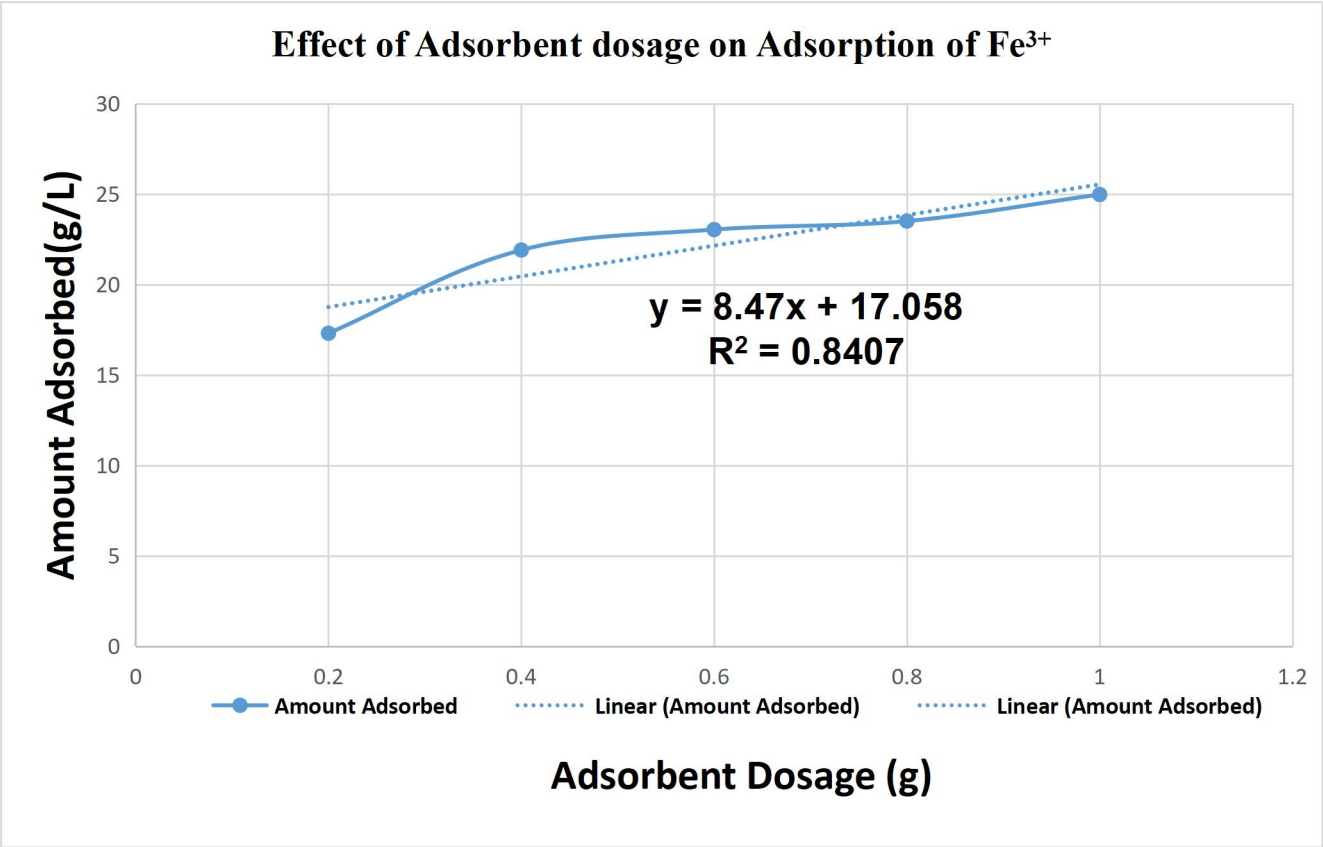

Fig 3.2: Effect of Adsorbent dosage on Adsorption of Fe^{3+} ion

DISCUSSION: EFFECT OF ADSORBENT DOSAGE

Increasing the mass of Aseni clay from 0.20 to 1.00 g (per 100 mL of 30 mg·L⁻¹ Fe^{3+}) produced a clear improvement in overall removal efficiency: percentage removal rose from 57.7% to 83.2% while the equilibrium concentration fell from 12.70 to 5.03 mg·L⁻¹. This pattern is typical for fixed-volume batch tests: adding more adsorbent increases the total number of

available binding sites and the probability of metal–site collisions, so the bulk removal improves. However, because the same total solute mass is shared across an increasing mass of adsorbent, the mass-normalized uptake (q_e) drops — a consequence of incomplete site utilization and distribution of the sorbate over more sorbent (Middea *et al.,* 2024).

The decline in q_e with dosage can also result from particle aggregation or overlap of adsorption sites at higher solid loadings, which reduces the effective surface area per unit mass and causes some sites to remain unsaturated. Intraparticle diffusion limitations can further moderate uptake per gram as dosage rises. Practically, the data suggest an operational trade-off: a higher dosage gives greater bulk removal (useful for polishing) but at lower adsorbent efficiency per gram; optimisation (minimum dosage that meets removal target) or activation/treatment of the clay is recommended if maximizing q_e is required (Orucoglu *et al.,* 2022; Maged *et al.,* 2023).

3.1.2 TABLE 3.3: EFFECT OF AGITATION TIME ON ADSORPTION OF Fe^{3+} ION

S/N	AGITATION TIME (MINS)	INITIAL CONC (mg/L)	EQUILIBRIUM CONC (mg/L)	AMOUNT ADSORBED (mg/L)	ADSORPTION CAPACITY (qe)	PERCENTAGE ADSORPTION (mg/L)
1	5	30	7.03	22.97 $\pm$0.76	2.30	76.57
2	15	30	5.87	24.13 $\pm$0.69	2.41	80.43
3	30	30	4.93	25.07 $\pm$0.65	2.51	83.57
4	60	30	4.77	25.23	2.52	84.10

				±0.12		
5	90	30	4.47	25.53 ±0.45	2.55	85.10
6	120	30	3.97	26.03 ±1.17	2.60	86.77

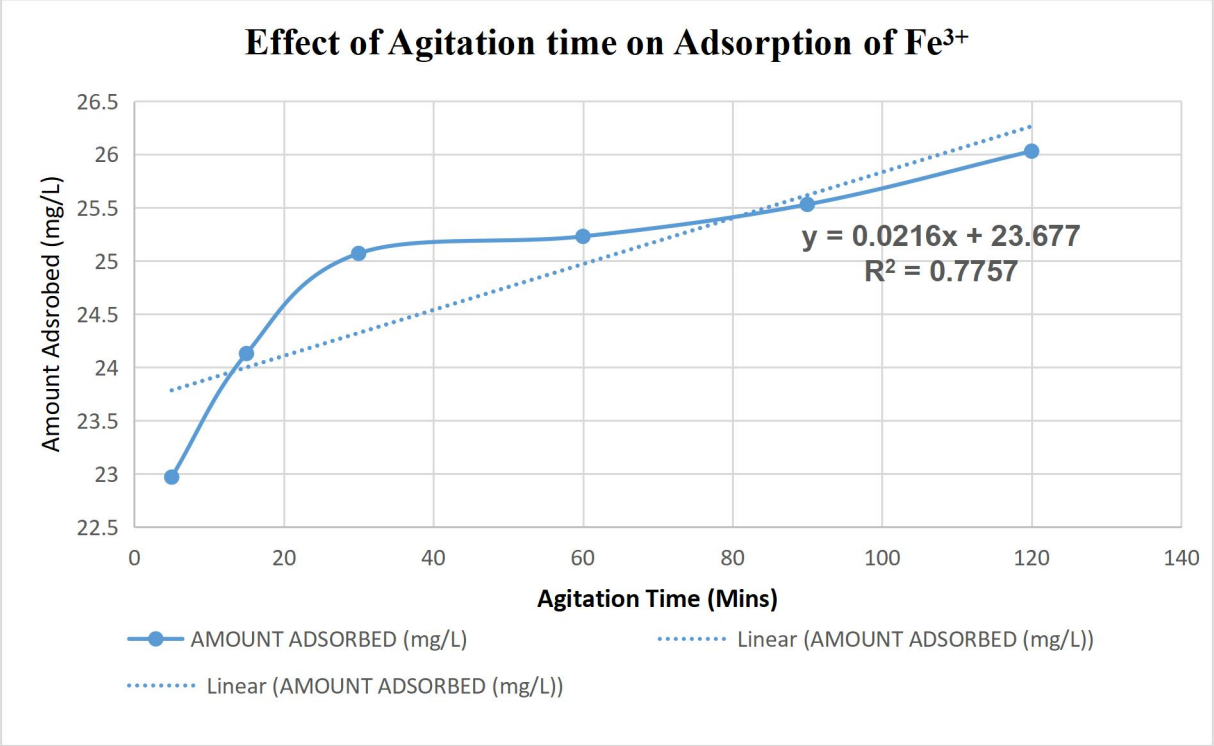

Fig 3.3: Effect of Agitation time on Adsorption of Fe^{3+}

DISCUSSION: EFFECT OF AGITATION TIME

The amount of Fe^{3+} adsorbed by Aseni clay increased with agitation time, rising from 22.97 $mg \cdot L^{-1}$ at 5 min to 26.03 $mg \cdot L^{-1}$ at 120 min, with most of the uptake occurring within the first 30–60 min. This two-stage pattern — a rapid initial uptake followed by a slower approach to equilibrium — is typical for metal adsorption onto clays: rapid external-surface binding occurs first, driven by a large concentration gradient, then slower intraparticle diffusion into pores and internal sites becomes rate-limiting as the system approaches

equilibrium (amount adsorbed trend) (Wang, P *et al.,* 2024)

The near-plateau between 60 and 120 min indicates that equilibrium is effectively reached by 90–120 min under these experimental conditions; therefore a contact time in that range is appropriate for batch tests with this clay and these concentrations. Similar contact-time behaviour has been observed for natural clays and clay-derived adsorbents in recent open-access studies, which also highlight that particle size, porosity, and site heterogeneity control the transition from fast surface uptake to slower diffusion-limited uptake (practical implication: choose 90–120 min for equilibrium runs or fit a kinetic model to quantify the diffusion contribution). (Mokokwe, G *et al.,*2022; Van Groeningen, N *et al.,* 2020)

3.1.3 TABLE 3.4: EFFECT OF pH ON ADSORPTION OF Fe^{3+} ION

S/N	pH	INITIAL CONC (mg/L)	EQUILIBRIUM CONC (mg/L)	AMOUNT ADSORBED (mg/L)	ADSORPTION CAPACITY (qe)	PERCENTAGE ADSORPTION (%)
1	4	100	0.37	99.63±0.12	9.96	99.63
2	5	100	0.27	99.73±0.06	9.97	99.73
3	6	100	0.33	99.67±0.12	9.97	99.67
4	7	100	0.40	99.60±0.20	9.96	99.60
5	8	100	0.30	99.70±0.10	9.97	99.70

6	9	100	0.17	99.83±0.06	9.98	99.83

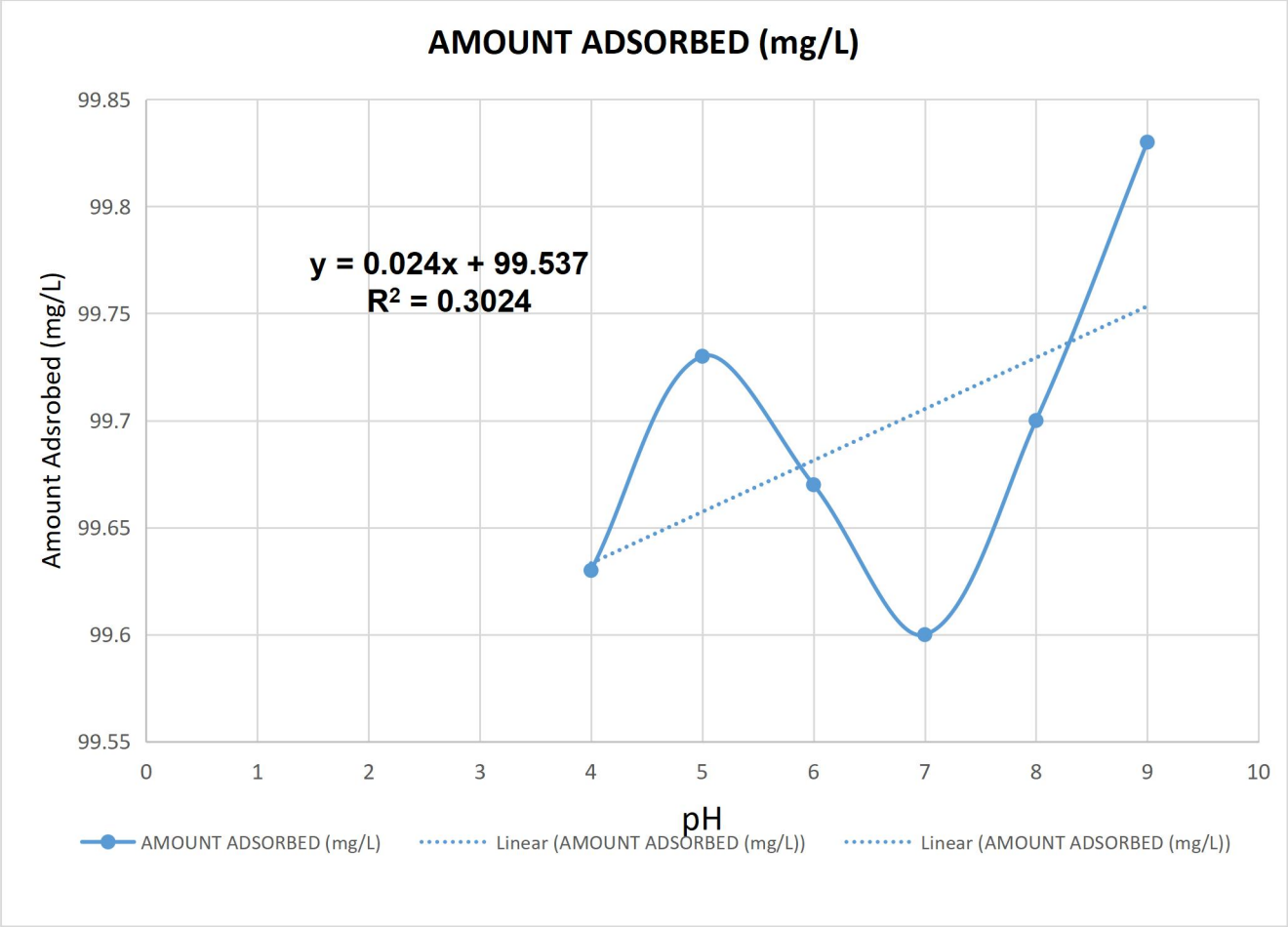

Fig 3.4: Effect of pH on Adsorption of Fe^{3+} ion

DISCUSSION: EFFECT OF pH

The data in Table 4 show extremely high apparent removals (≈99.63–99.8 %) across pH 4–9. Although at first glance this suggests exceptionally strong uptake by Aseni clay, the experimental observation that Fe^{3+} ion precipitated on addition of base (NaOH) indicates that the recorded decrease in dissolved Fe is mostly, or in large part, due to chemical precipitation of iron hydroxides rather than sorption onto the clay surface. Ferric iron is highly prone to hydrolysis: as pH increases the soluble Fe^{3+} species rapidly convert to hydrolysed forms and ultimately to insoluble $Fe(OH)_3(s)$. Thus, raising the pH

during the experiment can remove Fe from solution by precipitation, producing very low equilibrium concentrations that will be read by AAS as "high removal" but do not reflect surface adsorption capacity (Furcas *et al.,* 2024; Damato *et al.,* 2022).

Because precipitation and adsorption both remove metal from the dissolved phase but have different environmental implications, the pH series must be interpreted with care. To separate the two processes researchers commonly (a) keep the pH range below the onset of significant Fe^{3+} hydrolysis when studying sorption (often ≤ ~4–6 depending on ionic strength and complexation), (b) collect and analyze both dissolved and particulate fractions (for example, measure total Fe after acidifying samples to re-dissolve hydroxide precipitates, or analyze the filtered solids separately), and (c) use speciation/precipitation modeling or complementary analyses (e.g., XRD/SEM of solids) to confirm whether the removed iron is present as adsorbed species or as an precipitate (Furcas *et al.,* 2024; Damato *et al.,* 2022; Orucoglu *et al.,* 2022). Given the observation of immediate precipitation at pH 9, the pH-series results should be reported with the explicit caveat that the measured decrease in dissolved Fe at higher pH is confounded by hydroxide precipitation; values in Table 4 therefore do not provide reliable q_e values for adsorption without additional tests to quantify and/or re-dissolve precipitated iron.

During pH regulation of the Fe^{3+} solution prepared from $FeCl_3 \cdot 6H_2O$, the pH meter failed to display stable readings below pH 3 until sufficient base was added. This effect is attributed to the acid error of glass electrodes in strongly acidic media, where excessive H^+ activity saturates the electrode membrane, leading to inaccurate potentials. Moreover, Fe^{3+} ions in such conditions form hydrolyzed species like $[Fe(H_2O)_6]^{3+}$, which increase ionic strength and interfere with electrode response (Middea *et al.,* 2024). Consequently,

meaningful pH readings were only obtained after partial neutralization, as extreme acidity and ferric ion hydrolysis can distort pH measurement and affect adsorption equilibrium.

3.2 ADSORPTION ISOTHERM

3.2.1 TABLE 3.5: LANGMUIR ADSORPTION ISOTHERM RELATIONSHIP FOR Fe^{3+}

S/N	Co(mg/l)	Ce(mg/l)	Ca(mg/l)	V(L)	q_e $(\frac{mg}{g})$	$\frac{C_e}{q_e}(\frac{L}{g})$
1	10	0.43	9.57	0.1	0.96	0.45
2	20	1.70	18.30	0.1	1.83	0.93
3	30	4.57	25.43	0.1	2.54	1.80
4	40	10.17	29.83	0.1	2.98	3.41
5	50	13.80	36.20	0.1	3.62	3.81

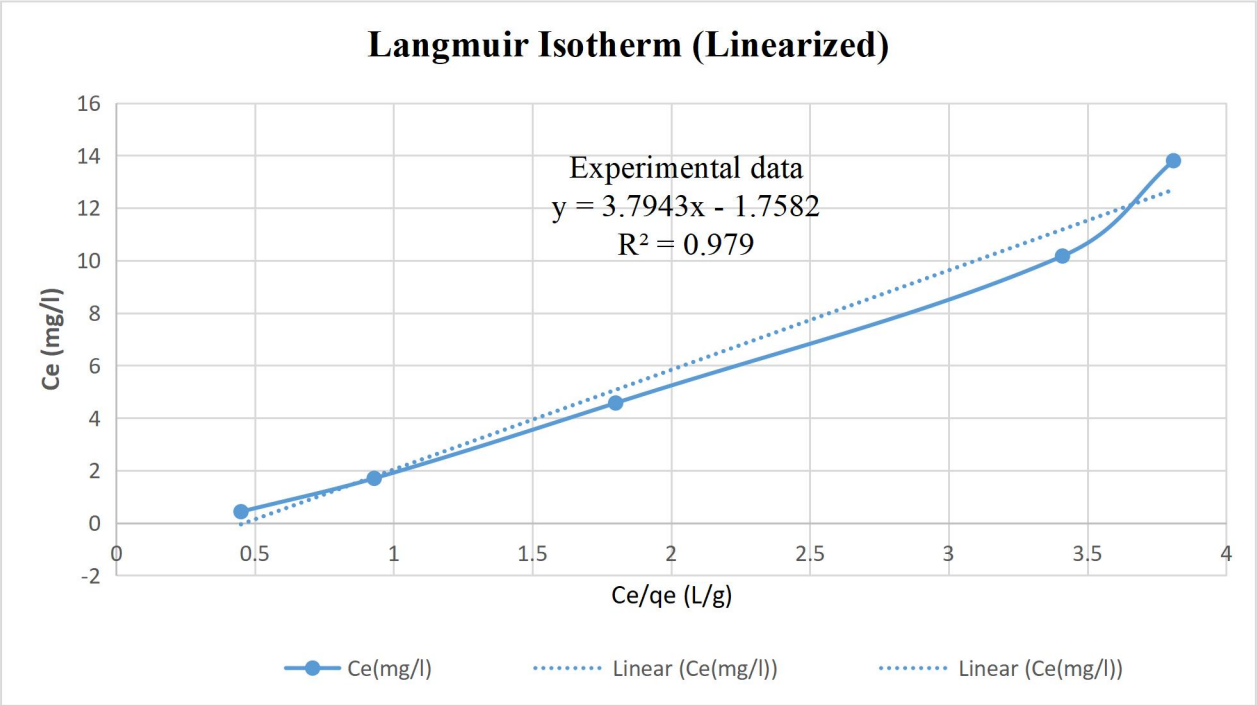

Fig 3.5: Langmuir Adsorption isotherm curve for Fe^{3+} ***ion***

DISCUSSION: LANGMUIR ADSORPTION ISOTHERM

The linearized Langmuir plot for Fe^{3+} adsorption on Aseni clay is described by the equation

$$\frac{Ce}{qe} = \frac{1}{\text{KLQm}} + \frac{Ce}{Qm},$$

$$\frac{Ce}{qe} = 3.7943Ce + 1.7582 \text{ with } R^2 = 0.979.$$

From this relationship (where slope $= 1/Q_m$ and intercept $= 1/(K_L Q_m)$), the derived Langmuir parameters are:

- Monolayer adsorption capacity,

$$Q_m = \frac{1}{\text{slope}} = \frac{1}{3.7943} = 0.264mg$$

.

Langmuir affinity constant, $K_L = \frac{1}{\text{intercept} \times Q_m} = \frac{1}{1.7582 \times 0.264} = 2.16L$

The relatively high correlation coefficient (R^2 = 0.979) indicates a good fit to the Langmuir model, suggesting that Fe^{3+} adsorption on Aseni clay largely occurs as a monolayer on a homogenous surface with finite identical active sites. The positive value of KL also implies a favorable adsorption process with strong interactions between the Fe^{3+} ions and the clay surface. The calculated K_L(≈2.16 L·mg^{-1}) implies a relatively strong affinity between Fe^{3+} and the clay surface under the experimental conditions. The low Qm value, however, may reflect the limited availability of surface sites or the competition between surface complexation and ion exchange processes typical of natural clays.

These observations are consistent with earlier studies on Fe^{3+} and heavy metal adsorption by natural clay minerals, which reported that Langmuir models effectively describe adsorption onto uniform active sites before surface saturation occurs (Middea *et al.,* 2024; Maged *et al.,* 2023; Orucoglu *et al.,* 2022). The close agreement between experimental data and the Langmuir prediction also supports the assumption of monolayer coverage, highlighting the strong binding affinity and structural suitability of Aseni clay for Fe^{3+} removal from aqueous solutions.

3.2.2 TABLE 3.6: FREUNDLICH ADSORPTION ISOTHERM RELATIONSHIP FOR Fe^{3+} ION

S/N	$q_e \frac{(mg)}{(g)}$	Log q_e	Ce(mg/l)	Log C_e
1	0.96	-0.02	0.43	-0.37

2	1.83	0.26	1.70	0.23
3	2.54	0.40	4.57	0.66
4	2.98	0.47	10.17	1.01
5	3.62	0.56	13.8	1.14

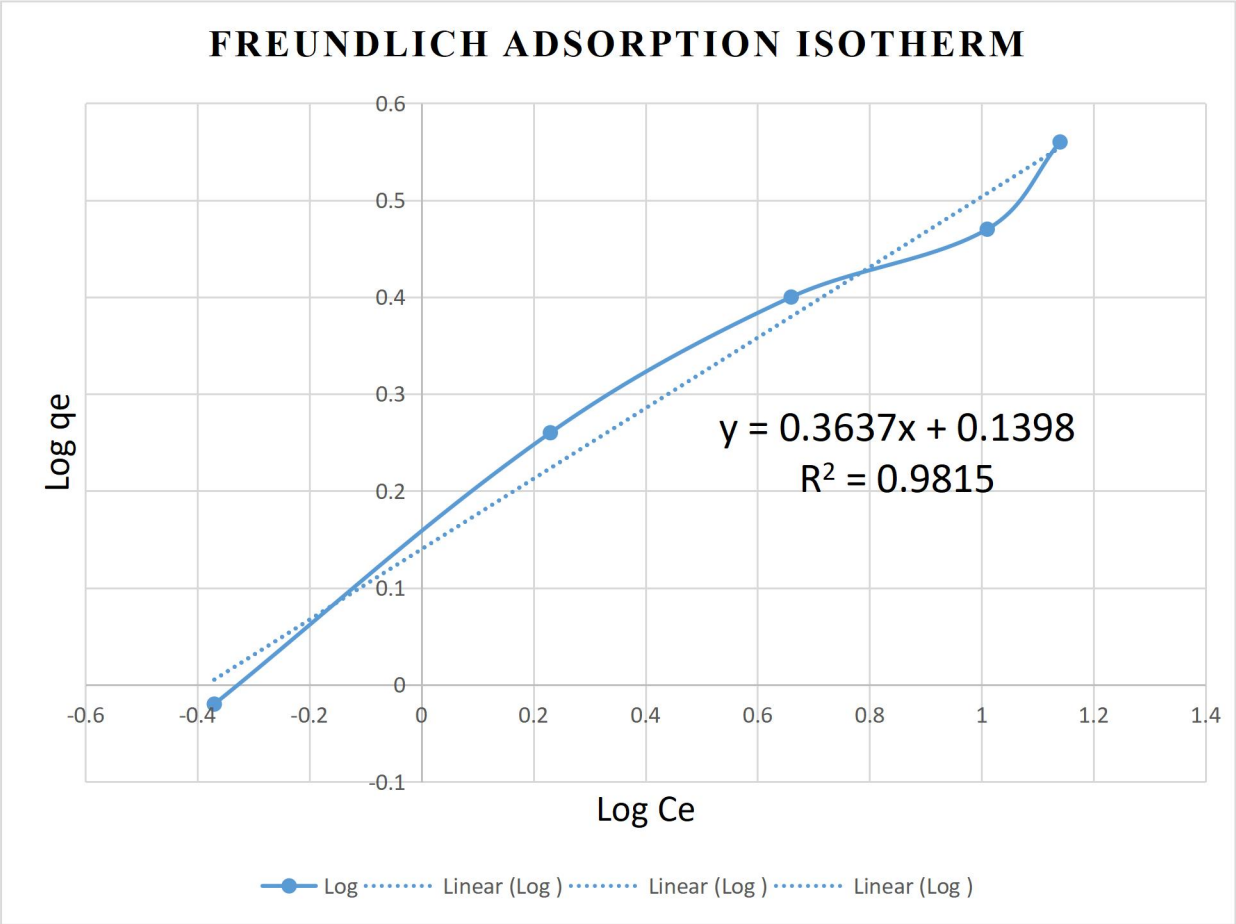

Fig 6: Freundlich Adsorption isotherm curve for $\mathbf{Fe^{3+}}$ ion

DISCUSSION: FREUNDLICH ADSORPTION ISOTHERM

The Freundlich adsorption isotherm for Fe^{3+} adsorption on Aseni clay is expressed by the linear equation $\log q_e = 0.3637 \log C_e + 0.1398$ with a coefficient of determination (R^2) of 0.9815.

The slope of the plot (1/n = 0.3637) and intercept ($\log K_f = 0.1398$) yield the Freundlich constants:

$$n = \frac{1}{0.3637} = 2.75, K_f = 10^{0.1398} = 1.38$$

The value of $n > 1$ signifies a favourable adsorption process, indicating that Fe^{3+} ions interact strongly with the heterogeneous surface of Aseni clay, with multiple types of adsorption sites contributing to the uptake. The moderately high correlation coefficient ($R^2 = 0.9815$) shows an excellent fit to the Freundlich model, suggesting that the adsorption process does not occur through uniform monolayer coverage as assumed by Langmuir, but rather through multilayer adsorption on energetically diverse sites.

These results further imply that the clay surface possesses varying affinities for Fe^{3+} ions, and as concentration increases, more active sites become available for sorption until equilibrium is reached. Similar findings have been observed in other studies involving natural clays and iron adsorption systems, where the Freundlich model better represented the heterogeneous and multilayer nature of adsorption compared to the Langmuir model (Middea *et al.,* 2024; Maged *et al.,* 2023; Orucoglu *et al.,* 2022).

3.3 ADSORPTION KINETICS

3.3.1 TABLE 3.7: PSEUDO-FIRST ORDER KINETICS FOR Fe^{3+} ION

S/N	TIME (min)	Ct(mg/L)	qe(mg/g)	qt(mg/g)	qe-qt (mg/g)	In(qe-qt)
1	10	7.03	2.60	2.30	0.30	-1.20
2	30	5.87	2.60	2.41	0.19	-1.66
3	45	4.93	2.60	2.51	0.09	-2.41
4	60	4.77	2.60	2.52	0.08	-2.53

5	90	4.47	2.60	2.55	0.05	-3.00
6	120	3.97	2.60	2.60	0.00	____

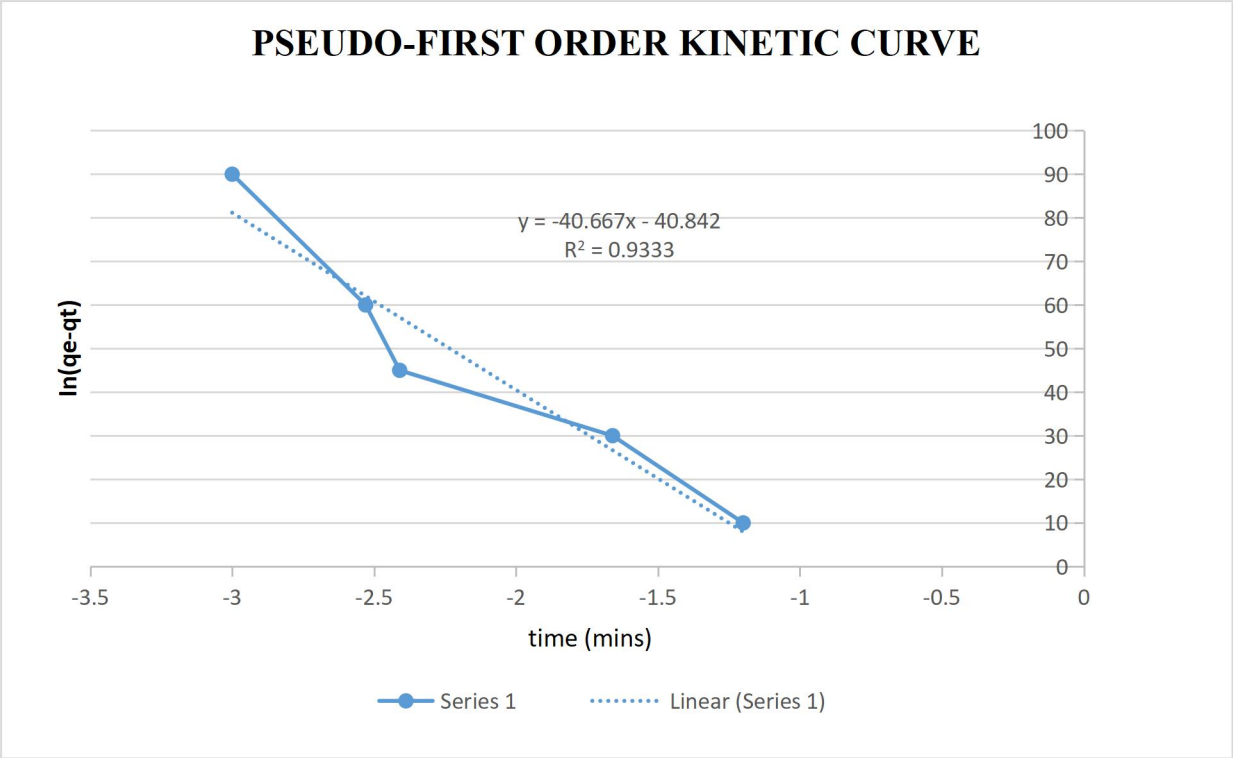

Fig 3.7: Pseudo-first order kinetic relationship - Fe^{3+} ion

DISCUSSION: PSEUDO FIRST ORDER KINETICS

The pseudo-first-order linear fit of $\ln(q_e - q_t)$ versus time produced the regression equation $\ln(q_e - q_t) = -0.0229t - 1.0814$ constant is $k_1 = 0.0529$ min^{-1} the coefficient of determination is $R^2 = 0.933$. this high R^2 value indicates that the model captures most of the time-dependent trend, and the relatively large k_1 implies a rapid uptake of Fe^{3+} onto the Aseni clay.

A slight deviation from ideal linearity was observed at longer contact times, which suggests that site heterogeneity or an additional (slower) step influences the approach to equilibrium.

Overall, the pseudo first order model provides a good, compact description of

the early and mid stages of adsorption, but the small nonlinearity at later time indicates that the process may not be governed solely by simple first-order behaviour.

3.3.2 TABLE 3.8: PSEUDO-SECOND ORDER KINETICS FOR Fe^{3+} ION

S/N	TIME(min)	Ct(mg/L)	qt(mg/g)	$\frac{t}{qt}(min.\frac{g}{mg}$
1	5	7.03	2.30	2.17
2	15	5.87	2.41	6.22
3	30	4.93	2.51	11.95
4	60	4.77	2.52	23.81
5	90	4.47	2.55	35.29
6	120	3.97	2.60	46.15

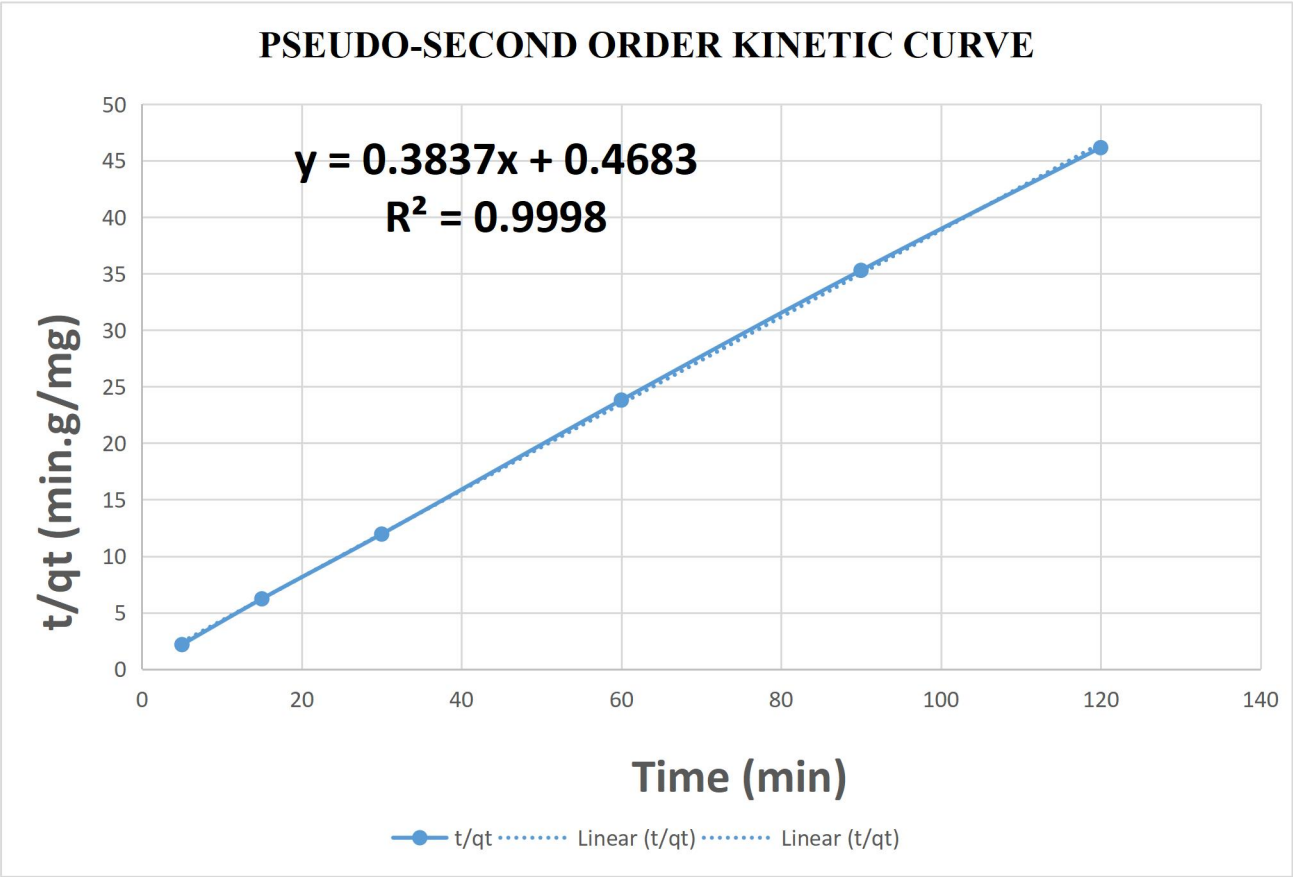

Fig 3.8: Pseudo-second order kinetic relationship - Fe^{3+} ion

DISCUSSION: PSEUDO SECOND ORDER KINETICS

standard linearized pseudo-second-order equation:

$$\frac{t}{q_t} = \frac{1}{k_2 q_e^2} + \frac{1}{q_e} t$$

The least-squares fit of t/q_t vs t gave:

- Linear equation:

$$\frac{t}{q_t} = (0.3837)\, t + 0.4683$$

Slope = 0.383687 (this equals $1/q_e$)

Intercept = 0.468339(this equals $1/(k_2 q_e^2)$

Coefficient of determination: $R^2 = 0.99976$(excellent linear fit)

From slope and intercept we calculate the kinetic parameters:

- $q_e = 1/\text{slope} = 1/0.383687 = 2.606$
- $k_2 = \frac{1}{\text{intercept} \times q_e^2} = \frac{1}{0.468339 \times (2.606)^2} = 0.3143$

The pseudo-second-order model produced an excellent linear fit for Fe^{3+} adsorption on Aseni clay, described by the equation $\frac{t}{q_t} = 0.3837\,t + 0.4683$ with $R^2 = 0.99976$. The high R^2 value (0.99976) confirms that the pseudo-second-order model better describes the adsorption process than the pseudo-first-order model, suggesting that chemisorption is the predominant mechanism governing Fe^{3+} uptake on Aseni clay. This implies that adsorption involves electron sharing or exchange between Fe^{3+} ions and active functional groups on the clay surface (Raji *et al.,* 2023). The excellent linearity further indicates that the adsorption process proceeds through valence forces, possibly via complexation or surface ion exchange, rather than mere physical interaction (Abbou *et al.,* 2021).

Similar findings have been reported in other studies of Fe^{3+} and heavy-metal adsorption onto clay minerals and modified natural adsorbents, where the pseudo-second-order model consistently provided the best fit due to the strong binding affinity of active sites and slow surface reaction kinetics (Gupta *et al.,* 2021). Therefore, the adsorption kinetics of Fe^{3+} on Aseni clay can be attributed to chemisorption controlled by the availability and reactivity of surface hydroxyl and silicate groups.

3.4 COMPARISON WITH PREVIOUS STUDY

The adsorption performance of Aseni clay for Fe^{3+} was evaluated through both equilibrium and kinetic studies, and the results were compared with previous findings in open-access literature. The adsorption data conformed well to both Langmuir and Freundlich models; however, the Freundlich model provided a slightly better fit (R^2 = 0.9815) than the Langmuir model (R^2 = 0.979). This suggests that adsorption occurred on a heterogeneous surface with varying site energies, which is typical of natural clays. Such behaviour indicates multilayer adsorption rather than uniform monolayer coverage, as is often observed in heterogeneous adsorbents. Studies have similarly reported better conformity of natural clays to the Freundlich model due to their heterogeneous pore structures and variable surface energies (Ayawei *et al.,* 2020; Wang *et al.,* 2024).

The Langmuir linearized equation for Fe^{3+} adsorption on Aseni clay was expressed as Ce/qe=3.7943Ce+1.7582 with an R^2 value of 0.979. From this relationship, the monolayer adsorption capacity (Q_m) and Langmuir affinity constant (K_L) were calculated as 0.264 $mg \cdot g^{-1}$ and 2.16 $L \cdot mg^{-1}$, respectively. These values indicate that Aseni clay possesses moderate adsorption affinity and limited active surface sites compared with more porous or chemically modified clays. Middea et al. (2024) reported higher monolayer capacities for natural palygorskite (up to 60 $mg \cdot g^{-1}$), demonstrating that mineral composition and activation methods significantly influence adsorption efficiency. Similarly, Maged et al. (2023) emphasized that surface modification and activation of clay minerals enhance their adsorption capacities by increasing surface area and improving metal ion binding affinity.

Kinetic analysis revealed that the adsorption process followed the pseudo-second-order model, with an R^2 value of approximately 0.9997, indicating chemisorption as the rate-limiting step. This suggests that

adsorption involved valence forces through the sharing or exchange of electrons between Fe^{3+} ions and the functional groups on the clay surface. The pseudo-first-order model showed a relatively poor fit, confirming that the process was not controlled by simple physical diffusion. Chahar et al. (2023) and Wang et al. (2024) similarly reported that pseudo-second-order kinetics best describe metal ion adsorption on clay-based materials due to their strong chemical interactions and surface complexation effects.

Overall, the results confirm that Aseni clay exhibits effective Fe^{3+} adsorption, particularly at lower concentrations, with adsorption following the pseudo-second-order kinetic model and fitting better to the Freundlich isotherm. The findings are consistent with the behaviour of natural clay systems reported in open-access studies, reinforcing that the adsorption mechanism is largely chemisorptive and occurs over heterogeneous surface sites with variable energy distributions.

3.5 SUMMARY OF RESULT

The adsorption of Fe^{3+} ions onto Aseni clay was studied under varying experimental parameters including initial concentration, adsorbent dosage, agitation time, and pH. The results revealed that adsorption efficiency was strongly influenced by these factors.

An increase in initial Fe^{3+} concentration from 10 to 50 mg L^{-1} led to a rise in adsorption capacity (q_e) from 0.96 mg g^{-1} to 3.62 mg g^{-1}, accompanied by a decrease in percentage removal from 95.7 % to 72.4 %. This indicated progressive site saturation at higher concentrations. Adsorbent dosage showed a direct relationship with removal efficiency, increasing from 57.67 % at 0.2 g to 83.23 % at 1.0 g, suggesting greater availability of active surface sites.

Agitation time significantly affected adsorption, with the amount adsorbed

increasing from 22.97 mg L^{-1} at 5 minutes to 26.03 mg L^{-1} at 120 minutes, indicating rapid initial adsorption followed by gradual equilibrium. The effect of pH showed consistently high adsorption (>99 %) within the tested range, though minor variations were observed due to $Fe(OH)_3$ precipitation at higher pH values.

Equilibrium data were analyzed using Langmuir and Freundlich isotherms. The Freundlich model (R^2 = 0.9815) provided a better fit than the Langmuir model (R^2 = 0.979), indicating heterogeneous surface adsorption and possible multilayer formation. Kinetic analysis showed that the pseudo-second-order model accurately described the adsorption process, confirming that chemisorption was the rate-limiting mechanism.

Overall, Aseni clay demonstrated good potential for Fe^{3+} removal from aqueous solutions, particularly at lower concentrations, confirming its suitability as a low-cost natural adsorbent for wastewater treatment applications.

3.6 CONCLUSION

The adsorption study established that Aseni clay possesses significant potential for the removal of Fe^{3+} ions from aqueous solutions. The efficiency of adsorption was found to depend on key parameters such as initial metal ion concentration, adsorbent dosage, agitation time, and pH. The adsorption capacity increased with higher metal concentrations, while percentage removal improved with increased adsorbent dosage and longer contact time. Optimal adsorption occurred at near-neutral pH conditions, although precipitation effects were observed at higher pH values.

The Freundlich isotherm provided a better fit for the equilibrium data (R^2 = 0.9815) compared to the Langmuir model (R^2 = 0.979), indicating that the

adsorption of Fe^{3+} ions occurred on a heterogeneous surface through multilayer interactions. Furthermore, the adsorption kinetics followed the pseudo-second-order model, suggesting that chemisorption was the dominant mechanism controlling the rate of adsorption.

Overall, the findings demonstrate that Aseni clay can serve as an efficient, low-cost, and environmentally friendly adsorbent for iron ion removal from contaminated water. The study provides a scientific basis for its potential use in wastewater treatment applications, particularly for communities where access to advanced treatment systems is limited.

3.7 RECOMMENDATON

- Further investigations should be carried out on the regeneration and reusability of Aseni clay to determine its long-term adsorption capacity and cost-effectiveness.
- Surface characterization techniques such as FTIR, SEM, and BET should be employed to better understand the functional groups, surface morphology, and pore structure responsible for Fe^{3+} adsorption.
- Adsorption experiments should be extended to real industrial wastewater samples to evaluate the performance of Aseni clay in complex environmental systems.
- Optimization studies should include parameters such as temperature, ionic strength, and the influence of competing ions to provide a more comprehensive understanding of the adsorption mechanism.
- Pilot-scale and community-based applications of Aseni clay should be explored as a sustainable and low-cost option for heavy metal removal in water treatment systems.

REFERENCES

Abbou, B., Aguedal, H., Ouchtou, H., Tounsadi, H., & Lahrichi, A. (2021). Removal of Cd(II), Cu(II), and Pb(II) by adsorption onto clay mineral-based materials: Kinetics and mechanism. *Applied Clay Science.* https://pmc.ncbi.nlm.nih.gov/articles/PMC8164196/

Abd Elnabi, A. H., El-Bialy, E. M., Elbanna, T. A., & Abdelhameid, A. H. (2023). Toxicity of heavy metals and recent advances in their remediation. Frontiers in Environmental Science, 11, 10384455. https://pmc.ncbi.nlm.nih.gov/articles/PMC10384455/

Abiodun, O.-A. O., Adeniyi, O. D., Adebayo, M. A., & Mustapha, A. T. (2023). Remediation of heavy metals using biomass-based adsorbents: Adsorption kinetics and isotherm models. Clean Technologies, 5(3), 881–899. https://doi.org/10.3390/cleantechnol5030047

Achievers University. (2023). Assessment of Nigerian clays for environmental remediation. Achievers University Publications. https://publications.achievers.edu.ng/publications/152/R6BCrSj9Zmb8.pdf

Akinyeye, R. O., Ogunleye, O. O., & Akinwande, A. S. (2023). Natural clays as sustainable adsorbents for heavy metal removal from aqueous solutions: A review. Heliyon, 9(3), e14123. https://doi.org/10.1016/j.heliyon.2023.e14123

Andrews, N. C., & Schmidt, P. J. (2007). Iron homeostasis. Annual Review of Physiology, 69, 69–85. https://doi.org/10.1146/annurev.physiol.69.031905.164337

Ayawei, N., Ebelegi, A. N., & Wankasi, D. (2020). Modelling and interpretation of adsorption isotherms. Journal of Chemistry, 2020, Article 3030617. https://doi.org/10.1155/2020/3030617

Bacon, J. R., Marshall, J., & Hill, S. J. (2021). Atomic spectrometry update: Review of advances in environmental analysis. Journal of Analytical Atomic Spectrometry, 36(1), 1–29. https://doi.org/10.1039/D0JA90074E

Bello, O. S., Adegoke, K. A., & Akinyunni, O. O. (2022). Preparation and characterization of a novel adsorbent from plantain peel for the removal of heavy metals from aqueous solution. Scientific African, 15, e01114. https://doi.org/10.1016/j.sciaf.2022.e01114

Bhatnagar, A., & Sillanpää, M. (2022). Advances in adsorption of heavy metals using low-cost adsorbents: A review. Journal of Water Process Engineering, 48, 102881. https://doi.org/10.1016/j.jwpe.2022.102881

Britannica. (2025). Clay mineral — Structure and classification. Encyclopedia Britannica. https://www.britannica.com/science/clay-mineral

Britannica. (2025). Iron: Properties and applications. Encyclopedia Britannica. https://www.britannica.com/science/iron-chemical-element

Camaschella, C. (2019). Iron deficiency and iron overload. New England Journal of Medicine, 381(19), 1901–1914. https://doi.org/10.1056/NEJMra1904781

Calori, S., Conti, F., Sabbadini, M. G., et al. (2023). Overview of ankle arthropathy in hereditary hemochromatosis. Reumatismo. https://pmc.ncbi.nlm.nih.gov/articles/PMC10443289/

Chahar, M., Kumar, V., Sharma, R., & Singh, J. (2023). Recent advances in the effective removal of hazardous contaminants using clay–polymer

nanocomposites. *Frontiers in Environmental Science, 11,* 1226101. https://www.frontiersin.org/articles/10.3389/fenvs.2023.1226101/full

Clay Minerals Society. (2020). The clay minerals glossary / nomenclature. Clay Minerals Society. https://www.clays.org/cms_nomenclature_glossary_april_2020_part_2_/

Damato, A., Vianello, F., Novelli, E., Balzan, S., et al. (2022). Comprehensive review on the interactions of clay minerals with animal physiology and production. Frontiers in Veterinary Science, 9, 9127995. https://www.ncbi.nlm.nih.gov/pmc/articles/PMC9127995/

El-Gendy, A. H., Al-Awadhi, M. M., El-Maghrabi, H. H., & Mostafa, A. M. (2022). Efficient removal of toxic heavy metals on kaolinite-based clay: Functional group insights by FTIR. Water, 17(13), 1938. https://doi.org/10.3390/w17131938

European Association for the Study of the Liver (EASL). (2022). EASL Clinical Practice Guidelines on haemochromatosis. Journal of Hepatology, 77(2), 479–502. https://www.journal-of-hepatology.eu/article/S0168-8278(22)00211-2/fulltext

Fabio, E. F., Mundra, S., Lothenbach, B., & Angst, U. M. (2024). Chloride binding in cementitious systems: Influence of hydration, carbonation, and microstructure. *Environmental Science & Technology, 58*(44), 19851–19860. https://doi.org/10.1021/acs.est.4c06818

Furcas, F. E., Mundra, S., Lothenbach, B., & Angst, U. M. (2024). Speciation controls the kinetics of iron hydroxide precipitation and transformation at alkaline pH. Environmental Science & Technology, 58, 19851–19860. https://doi.org/10.1021/acs.est.4c06818

Ganz, T., & Nemeth, E. (2021). Iron homeostasis in host defence and inflammation. Nature Reviews Immunology, 21, 374–386. https://www.nature.com/articles/s41577-020-00432-5

Girelli, D., Busti, F., & Camaschella, C. (2024). Diagnosis and management of hereditary hemochromatosis. Haematologica, 109(6), 1551–1562. https://pmc.ncbi.nlm.nih.gov/articles/PMC11665571/

Goodenough, J. B., & Park, K.-S. (2013). The Li-ion rechargeable battery: A perspective. Journal of the American Chemical Society, 135(4), 1167–1176. https://doi.org/10.1021/ja3091438

Greenwood, N. N., & Earnshaw, A. (2012). Chemistry of the elements (2nd ed.). Elsevier.

Gu, Z., Deng, B., Yang, J., & Gang, D. D. (2019). Clay mineral adsorbents for heavy metal removal from wastewater: A review. Environmental Chemistry Letters, 17, 629–654. https://doi.org/10.1007/s10311-018-0813-9

Gupta, V. K., & Gupta, M. (2022). Applications of iron salts in industry and environment: A review. Journal of Environmental Management, 314, 114922. https://doi.org/10.1016/j.jenvman.2022.114922

Hasan, H. A., Jamal, N., Sheikh Abdullah, S. R., Abu Bakar, S. N. H., Muhamad, M. H., & Li, X. (2021). Effective iron-accumulating bacteria isolated from chemical laboratory drainage for iron removal. Journal of

Ecological Engineering, 22(2), 187–194. https://doi.org/10.12911/22998993/131030

Hathaway, D., & Muthusamy, A. (2023). Siderosis. In StatPearls [Internet]. Treasure Island (FL): StatPearls Publishing. https://www.ncbi.nlm.nih.gov/books/NBK606098/

He, L., Zhang, J., Chen, D., & Liu, Y. (2024). Pollution characteristics and risk assessment of heavy metals in sediment of Dianchi Lake. Toxics, 12(5), 322. https://doi.org/10.3390/toxics12050322

Heliyon. (2023). RSM optimization studies for cadmium ions adsorption onto pristine and acid-modified kaolinite clay. Heliyon, 9(9), e19108.

Huang, J., Li, X., & Sun, Y. (2022). Iron oxide nanoparticles in biomedical applications: Progress and perspectives. Advanced Functional Materials, 32(14), 2107915. https://doi.org/10.1002/adfm.202107915

Ibrahim, S., Hussain, S., & Mahmud, H. (2021). Preparation and characterization of natural clay and its application in removal of Pb^{2+} and Cd^{2+} from wastewater. Applied Water Science, 11, 154. https://doi.org/10.1007/s13201-021-01461-y

Jomova, K., Alomar, S. Y., Nepovimova, E., Kuca, K., & Valko, M. (2024). Heavy metals: Toxicity and human health effects. Archives of Toxicology, 99(1), 153–209. https://doi.org/10.1007/s00204-024-03903-2

Kostoglou, M. (2022). Why is the linearized form of pseudo-second-order kinetics so widely used? *Processes (MDPI)*. https://www.mdpi.com/2504-5377/6/4/55

Kumari, P., Yadav, S., & Singh, A. (2021). Clay minerals: Structure, chemistry and significance in soil–plant interactions. Applied Clay Science, 213, 106231. https://doi.org/10.1016/j.clay.2021.106231

Li, Y., et al. (2019). Excess iron and oxidative stress in plants and implications for health. Plant Physiology and Biochemistry, 139, 1–12. https://doi.org/10.1016/j.plaphy.2019.04.031

Lide, D. R. (2004). CRC Handbook of chemistry and physics. CRC Press.

Liu, X., Tournassat, C., Grangeon, S., et al. (2022). Molecular-level understanding of metal ion retention in clay-rich materials. Nature Reviews Earth & Environment, 3, 461–476. https://doi.org/10.1038/s43017-022-00301-z

Maged, A., El-Fattah, H. A., Kamel, R. M., Ibrahim, M., & Elnour, M. (2023). A comprehensive review on sustainable clay-based geopolymers for wastewater treatment: Circular economy and future outlook. *Environmental Monitoring and Assessment, 195,* 617. https://pubmed.ncbi.nlm.nih.gov/37204517/

Mansouri, N., Merabet, S., & Khelifi, A. (2022). Adsorption of heavy metals from aqueous solutions by using natural clays: A review. Materials Today: Proceedings, 62, 3494–3500. https://doi.org/10.1016/j.matpr.2022.03.551

Mayo Clinic. (2025). Hemochromatosis: Symptoms and causes. Mayo Clinic. https://www.mayoclinic.org/diseases-conditions/hemochromatosis/symptoms-causes/syc-20351443

Middea, A., Spinelli, L. d. S., de Souza Junior, F. G., Fernandes, T. d. L. A. P., de Lima, L. C., Barthem, V. M. T. S., Gomes, O. d. F. M., & Neumann, R.

(2024). Removal of Fe^{3+} ions from aqueous solutions by adsorption on natural eco-friendly Brazilian palygorskites. Mining, 4(1), 37–57. https://doi.org/10.3390/mining4010004

Mokarram, R. R., Khezri, S. M., & Lin, D. (2022). Advances in adsorption kinetics and equilibrium modeling: Applications in environmental systems. Journal of Environmental Management, 316, 115251. https://doi.org/10.1016/j.jenvman.2022.115251

Mokokwe, G., Huma, L., Mooketsi, K., & Dhlamini, M. (2022). Investigation of clay brick waste for the removal of copper and other ions—Kinetic modelling and mechanism discussion. *Scientific Reports, 12,* 12643. https://www.ncbi.nlm.nih.gov/pmc/articles/PMC9304740/

Moustafa, M. T. (2023). Preparation and characterization of low-cost adsorbents for the efficient removal of malachite green using response surface modeling and reusability studies. Scientific Reports, 13, 4493. https://doi.org/10.1038/s41598-023-31391-4

Negrão, R., Andrade, J., & Maciel, A. (2023). Environmental monitoring of heavy metals in aquatic macrophytes by atomic absorption spectrometry. Applied Advances in Science, 4(1), 29–38. https://doi.org/10.54517/aas.v4i1.1972

Nkwunonwo, U. C., Odika, P. O., & Onyia, N. I. (2020). A review of the health implications of heavy metals in the food chain in sub-Saharan Africa. Scientific African, 8, e00337. https://doi.org/10.1016/j.sciaf.2020.e00337

Nkwunonwo, U. C., et al. (2020). A review of heavy metal pollution and remediation strategies in Nigeria. Journal of Health and Pollution, 10(28), 200605. https://doi.org/10.5696/2156-9614-10.28.200605

Orucoglu, E., Grangeon, S., Gloter, A., & Tournassat, C. (2022). Competitive adsorption processes at clay mineral surfaces: A coupled experimental and modeling approach. *ACS Earth and Space Chemistry, 6*(2), 211–223. https://doi.org/10.1021/acsearthspacechem.1c00323

Pennell, D. J., Carpenter, J.-P., et al. (2023). Iron overload cardiomyopathy. Circulation Research, 132(9), 1200–1219. https://www.ahajournals.org/doi/10.1161/CIRCRESAHA.123.321456

Pietrangelo, A. (2015). Hereditary hemochromatosis: Pathogenesis, diagnosis, and treatment. Gastroenterology, 149(5), 1240–1251. https://doi.org/10.1053/j.gastro.2015.06.013

Piperno, A. (2020). Inherited iron overload disorders. Translational Gastroenterology and Hepatology, 5, 25. https://tgh.amegroups.org/article/view/5608/htmlRastogi, A., Zivcak, M., Sytar, O., Kalaji, H. M., He, X., Mbarki, S., & Brestic, M. (2022). Impact of metal and metalloid toxicity on photosynthesis: Role of antioxidants. International Journal of Molecular Sciences, 23(2), 572. https://doi.org/10.3390/ijms23020572

Raji, Z., Karim, A., Karam, A., & Khalloufi, S. (2023). Adsorption of heavy metals: Mechanisms, kinetics, and applications of various adsorbents in wastewater remediation—A review. *Waste, 1*(3), 775–805. https://doi.org/10.3390/waste1030046

Royal Society of Chemistry (RSC). (2025). Iron – Element information, properties and uses. Royal Society of Chemistry. https://www.rsc.org/periodic-table/element/26/iron

Saad, N., et al. (2020). Pulmonary siderosis in an industrial worker—A case report. Respiratory Medicine Case Reports, 30, 101116. https://pmc.ncbi.nlm.nih.gov/articles/PMC7284170/

Sen, T. K. (2023). Agricultural solid wastes based adsorbent materials in the remediation of heavy metal ions from water and wastewater by adsorption: A review. Molecules, 28(14), 5575. https://doi.org/10.3390/molecules28145575

Singh, A., Kumari, P., & Yadav, S. (2021). Adsorption phenomena: Theory, mechanism and application in removal of pollutants. Applied Clay Science, 213, 106231. https://doi.org/10.1016/j.clay.2021.106231

Smith, J., Patel, R., & Zhang, H. (2021). Iron-based catalysts for sustainable chemical synthesis. Catalysis Today, 371, 152–165. https://doi.org/10.1016/j.cattod.2020.08.034

Soltaninejad, S., Marandi, S. M., & Nalbantoglu, B. P. (2023). Effects of the types and amounts of clay minerals on durability of lime-stabilized soils. Minerals, 13(10), 1317. https://doi.org/10.3390/min13101317

Szczerbińska, A., et al. (2024). Hemochromatosis—How not to overlook and properly diagnose it. Journal of Clinical Medicine, 13(13), 3660. https://www.mdpi.com/2077-0383/13/13/3660

Tibebe, B., Tsegaye, T., & Mulaw, T. (2022). Assessment of selected heavy metals in honey samples using flame atomic absorption spectroscopy in

Ethiopia. BMC Chemistry, 16(1), 31. https://doi.org/10.1186/s13065-022-00878-y

Tkachenko, R., & Niedzielski, P. (2022). FTIR as a method for qualitative assessment of solid samples in geochemical research: A review. Molecules, 27(24), 8846. https://doi.org/10.3390/molecules27248846

Tran, H. N., Tomul, F., Ha, N. T., Nguyen, D. T., Lima, E. C., Le, G. T., … & Woo, S. H. (2021). Innovative spherical biochar for pharmaceutical removal from water: Insight into adsorption mechanism. Journal of Hazardous Materials, 414, 125493. https://doi.org/10.1016/j.jhazmat.2021.125493

Van Groeningen, N., Müller, F., Hülsemann, M., & Kosmulski, M. (2020). Interactions of ferrous iron with clay mineral surfaces during redox processes. *Environmental Monitoring and Chemistry.* https://pubs.rsc.org/en/content/articlehtml/2020/em/d0em00063a

Wang, H., Chen, Y., Zhang, J., & Chen, H. (2024). Natural clay minerals as efficient adsorbents for heavy metals: Progress and perspectives. Environmental Pollution, 329, 121707. https://doi.org/10.1016/j.envpol.2023.121707

Wang, L., Chen, Y., & Li, J. (2023). Recent developments in adsorption processes for environmental remediation. Environmental Science and Pollution Research, 30(15), 40221–40239. https://doi.org/10.1007/s11356-023-27445-2

Wang, P., Zhang, X., & Liu, Y. (2024). Clay-based materials for heavy metals adsorption: Mechanisms, advancements, and future prospects. *Crystals, 14*(12), 1046. https://www.mdpi.com/2073-4352/14/12/1046

Ward, R. J., Zucca, F. A., Duyn, J. H., Crichton, R. R., & Zecca, L. (2024). The role of brain iron in neurodegenerative disorders. Nature Reviews Neurology, 20, 541–558. https://www.nature.com/articles/s41582-024-01099-5

World Health Organization (WHO). (2020). Anaemia and iron deficiency. *World Health Organization